

## INACTIVATED BHV-1 AS AN IMMUNOTHERAPY

INACTIVE, BUT NOT INEFFECTIVE:  
THE THERAPEUTIC POTENTIAL OF NON-REPLICATING  
BOVINE HERPESVIRUS TYPE-1

By Enzo Mongiovi Baracuhy, B.Sc. Hons.

A Thesis Submitted to the School of Graduate Studies in Partial Fulfilment of the Requirements  
for the Degree Master of Science

McMaster University © Copyright by Enzo Mongiovi Baracuhy, April, 2024

McMaster University MASTER OF SCIENCE (2024) Hamilton, Ontario (Biochemistry & Biomedical Sciences)

TITLE: Inactive, but not ineffective: the therapeutic potential of non-replicating Bovine herpesvirus type-1

AUTHOR: Enzo Mongiovi Baracuh, B.Sc. (Hons., University of Guelph)

SUPERVISOR: Karen Mossman, Ph.D.

NUMBER OF PAGES: xi, 76

## **Abstract**

Viral immunotherapy is a promising approach for cancer treatment where viruses can selectively target and kill cancer cells while also stimulating an immune response. Among viruses with this ability, Bovine herpesvirus type-1 (BHV-1) has several advantages, including previous data suggesting it does not require viral replication for its anti-cancer effects. We have previously demonstrated that binding and penetration of enveloped virus particles are sufficient to trigger intrinsic and innate immune signalling. In addition, we have published data showing mutated herpesviruses with lower replication *in vitro* exhibit stronger anti-tumour activity *in vivo*. Experiments in established animal models comparing the survival of mice bearing melanoma C10 cells treated with either live or UV (non-replicating) BHV-1 show that both viruses similarly extend survival. Transcriptomic analysis of C10 cells and tumours treated with either live or UV-inactivated BHV-1 has revealed a subset of overlapping differentially regulated genes and similar pathway enrichments, suggesting live and UV BHV-1 have similar mechanisms of activity. Lastly, the infiltration patterns of various immune cells in tumours following treatment with live and UV BHV-1 show that both viruses induce similar proportions of the same populations of immune cells, with the exception of neutrophils. This work highlights the potential of non-replicating BHV-1 as an effective immunotherapy and suggests that viral replication may not be necessary for therapeutic efficacy. These findings contribute to our understanding of the mechanisms underlying BHV-1 immunotherapy and provide insights into the immune response elicited by both live and UV-inactivated BHV-1, paving the way for further development of BHV-1-based cancer treatments.

## **Acknowledgements**

First, of course, Dr. Karen Mossman. Words cannot begin to describe how appreciative I am of your support and care. One of my first impressions was how fast you are at replying to emails despite being the busiest person I have had the privilege of working with. I sometimes make the joke that you have a Wi-Fi router installed in your brain (do you?), because that is the only way someone could manage your day-to-day while still being such an attentive mentor. Thank you for being so flexible with meetings and deadlines, for your endless encouragement when I couldn't figure out my path, and of course, your guidance in helping me become a better scientist. As for my committee members Dr. Matthew Miller and Dr. Jonathan Bramson, thank you both for your insights that helped shape my project, and your honest sincere advice when I needed it most. Your wisdom(s) always gave me a lot to think about.

To Maria Davola, Olga Cormier, and Susan Collins (my lab aunties). I could not have gotten as far as I did without all of you backing me and up helping me plan and execute my experiments. Maria, I've never met anyone as informed and knowledgeable about mice. You always knew the right decision to make when I had problems and were there making sure I wasn't missing any steps in these long and complicated protocols. Asking people for life advice often ends in more questions than answers, but you were one of the few people who gave your honest opinions no matter how hard it may have been for me to hear, and that is something I truly appreciated. I am so grateful to have had you as my mentor these past two years. Olga, you might remember that when we first met I often forgot about our age difference, and that's because you made me feel like I was just talking to a friend I've had for years. I cannot express how helpful you were with your willingness to jump on zoom last minute when I had questions

about Clariom, reading my essays when I applied to programs (also last minute), and offering to help with experiments before I even asked. I always knew I could rely on your opinions. Susan, every time we speak, you continue to amaze me with how strong of a grasp and expertise you have on ... well, everything. I know for sure you could write textbooks upon textbooks on viruses and still have more to say. In the lab, I could not have gotten by without your never-ending patience when I made mistakes, had questions upon questions, or kept coming back with the same problem. Thank you for being so present and attentive, you truly are the backbone of this lab.

Thank you Mom and Dad for providing unquestioned support whenever I needed it. Your support of my education from when we first came to Canada to now in my university studies has pushed me forward and given me the motivation to succeed in academic environments. The sacrifices you made to uproot your lives and come to a new country with two young children continues to inspire me.

To my partner Evan Morin. While I don't say it often, your generosity does not go unnoticed. Thank you for carrying my weight when we lived downtown, and the countless hours you've spent carefully reading draft after draft of this document even though most of it is gibberish to you and you had big exams to study for. Thank you for being a listening ear when I had bad days and anxieties about the future, I always knew I could count on you to make me feel better.

To one of my best friends, Monique Ferreira. Being so wrapped up in science day in and day out, I truly cannot put a price on those weekends where I can just disconnect and spend time with you walking around Toronto and then coming back to my house to play Super Mario Bros. Trying new foods and putting aside my responsibilities for just a little with you was instrumental in keeping me going and focused throughout this journey. I can always count on a weekend with Mo to help me unwind.

I am eternally grateful for the challenges and growth I've experienced over these past two years. I've learned so much about my wants, needs, what I'm good at (and not good at), and look forward to taking on whatever is next. I will always cherish my time in the Mossman Lab.

## Table of Contents

<i>Abstract</i>	<i>ii</i>
<i>List of Figures and Tables</i>	<i>viii</i>
<i>List of Abbreviations</i>	<i>ix</i>
<i>Lay Abstract</i>	<i>xi</i>
<b>1. Introduction</b>	<b>1</b>
<b>1.1 Oncolytic viruses</b>	<b>1</b>
<b>1.2 The role of the immune response in oncolytic virotherapy</b>	<b>3</b>
1.2.1 Cellular sensing of viruses	3
1.2.2 The function of different immune cells	5
<b>1.3 Combination therapies</b>	<b>12</b>
<b>1.4 Bovine herpesvirus type-1</b>	<b>14</b>
<b>1.5 Is viral replication needed for an OV to be effective?</b>	<b>15</b>
<b>1.6 UV inactivation</b>	<b>18</b>
<b>1.7 Study objectives and hypothesis</b>	<b>19</b>
<b>1.8 Implications of this study</b>	<b>20</b>
<b>2 Materials and Methods</b>	<b>21</b>
<b>2.2 Cells</b>	<b>21</b>
<b>2.2 Viruses</b>	<b>21</b>
<b>2.3 Plaque assays</b>	<b>21</b>
<b>2.4 Growth curves</b>	<b>22</b>
<b>2.5 Optimizing conditions for heat inactivation</b>	<b>22</b>
<b>2.6 Optimizing conditions for UV inactivation</b>	<b>22</b>
<b>2.7 Quantitative RT-PCR</b>	<b>23</b>
<b>2.8 Transcriptome profiling</b>	<b>24</b>
<b>2.9 Drug and antibody preparation for <i>in vivo</i> experiments</b>	<b>25</b>
<b>2.10 Tumour regression of mice bearing C10 tumours treated with live or UV BHV-1</b>	<b>25</b>
<b>2.11 Tumour infiltration of immune cells</b>	<b>26</b>
<b>2.12 Statistical Analysis</b>	<b>26</b>
<b>3 Results</b>	<b>27</b>
<b>3.2 Developing an inactivated Bovine herpesvirus type-1 (BHV-1) platform</b>	<b>27</b>
3.2.2 Different temperatures and durations lead to heat inactivation of BHV-1	27
3.2.3 Treating BHV-1 at 70°C for 5 minutes does not affect overall virion structure	29
3.2.4 HI BHV-1 does not induce the expression of interferon-stimulated genes (ISGs)	30
3.2.5 UV-inactivating BHV-1 leads to a dose-dependent reduction in viral replication	31
3.2.6 UV-inactivated BHV-1 induces significantly more ISG expression compared to live BHV-1	33



<b>3.3</b>	<b>700mJ/cm<sup>2</sup> of UV is enough to inactivate BHV-1 at concentrations needed for <i>in vivo</i> experiments</b>	<b>34</b>
<b>3.4</b>	<b>UV BHV-1 is as effective as live BHV-1 at extending survival of tumour-bearing mice</b>	<b>36</b>
<b>3.5</b>	<b>Live and UV BHV-1-treated tumours have similar immune cell infiltration profiles</b>	<b>38</b>
<b>3.6</b>	<b>Live BHV-1 + Mitomycin C and UV BHV-1 + Mitomycin C-treated tumours have similar gene signatures and pathway enrichment profiles</b>	<b>40</b>
<b>3.7</b>	<b>Live BHV-1 + Mitomycin C and UV BHV-1 + Mitomycin C-treated C10 cells have similar gene signatures and pathway enrichment profiles</b>	<b>42</b>
<b>3.8</b>	<b>Only 16 genes comprise BHV-1’s “gene signature” in C10 cells across <i>in vitro</i> and <i>in vivo</i> models</b>	<b>44</b>
<b>3.9</b>	<b>Only a small subset of genes is differentially regulated in live and UV BHV-1-infected C10 cells.</b>	<b>47</b>
<b>4.</b>	<b><i>Discussion</i></b>	<b>49</b>
<b>4.1</b>	<b>UV BHV-1 as the chosen platform inactivation vector</b>	<b>49</b>
<b>4.2</b>	<b>Regression of tumours treated with live and UV BHV-1</b>	<b>52</b>
<b>4.3</b>	<b>Analysis of Tumour-infiltrating Immune Cells</b>	<b>53</b>
<b>4.4</b>	<b>The transcriptome of cells and tumours treated with live versus UV BHV-1</b>	<b>56</b>
<b>5.</b>	<b><i>Conclusion</i></b>	<b>61</b>
	<b><i>Appendix: Arabinofuranosyl Cytidine (AraC) as a drug to produce BHV-1 L-particles</i></b>	<b>62</b>

## **List of Figures and Tables**

Figure 1. Optimization of BHV-1 heat-inactivation. ....	28
Figure 2. Size distribution of live and oBHV-1 inactivated at 70°C for 5 min.....	29
Figure 3. Heat-inactivated BHV-1 fails to induce interferon-stimulated gene (ISG) expression in C10 cells at 6hpi.....	30
Figure 4. Effect of different UV intensities on BHV-1 replication. ....	32
Figure 5. Induced expression of ISGs in C10 cells after infection with live and UV BHV-1 at 6hpi. ....	33
Figure 6. Plaque assay and growth curve analysis of live and UV-Inactivated BHV-1.....	35
Figure 7. UV-BHV-1 is as effective as live BHV-1 at extending the survival of mice bearing C10 melanoma tumours.....	37
Figure 8. Tumour infiltration profile of tumours treated with either live or UV BHV-1.....	39
Figure 9. Pathway enrichment profiles and differentially regulated genes of tumours treated with Mitomycin C and either live or UV BHV-1. ....	41
Figure 10. Pathway enrichment profiles and differentially regulated genes of C10 (B16-hN1) cells treated with Mitomycin C and either live or UV BHV-1 at 12hpi. ....	43
Figure 11. Schematic diagram of differential gene expression patterns (>3-fold) in C10 (B16-hN1) cells and tumours infected <i>in vitro</i> (12hpi) or <i>in vivo</i> (5dpi) with live or UV oBHV-1 in the presence of low dose mitomycin C (Mito). ....	45
Table 1. Summarized roles of the 16 "Signature" genes.....	46
Figure 12. Differential gene expression patterns in C10 cells infected with UV and live BHV-1 in the presence of DMSO.....	48
Figure 13. Effect of arabinofuranosyl cytidine (AraC) on BHV-1 replication.....	64
Figure 14. Concentration optimization of custom VP8 and VP5 antibodies.....	65
Figure 15. Western blots targeting the major capsid protein VP5 and major tegument protein VP8. ....	66

## **List of Abbreviations**

<b>ADAR</b>	Adenosine Deaminase Acting on RNA
<b>BHV-1</b>	Bovine herpesvirus type-1
<b>BMP</b>	Bone morphogenetic protein
<b>CCL-2</b>	Chemokine C-C motif ligand 2
<b>CD</b>	Cluster of Differentiation
<b>cGAS</b>	Cyclic GMP-AMP synthase
<b>Cmpk2</b>	Cytidine monophosphate kinase 2
<b>CTLA-4</b>	cytotoxic T-lymphocyte associated protein 4
<b>CXCL10</b>	C-X-C motif chemokine ligand 10
<b>DAMP</b>	Death-associated molecular pattern
<b>DCs</b>	Dendritic cells
<b>DMEM</b>	Dulbecco's Modified Eagle Medium
<b>dpi</b>	Days post-infection
<b>FBS</b>	Fetal Bovine Serum
<b>Gbp2</b>	Guanylate binding protein 2
<b>gD</b>	Glycoprotein D
<b>gE</b>	Glycoprotein E
<b>GFP</b>	Green fluorescent protein
<b>gI</b>	Glycoprotein I
<b>GM-CSF</b>	Granulocyte-macrophage colony-stimulating factor
<b>HI</b>	Heat-inactivated
<b>HSV-1</b>	Herpes simplex virus type-1
<b>ICD</b>	Immunogenic cell death
<b>ICI</b>	Immune checkpoint inhibitor
<b>ICP0</b>	Infected cell protein 0

<b>IFIT1</b>	Interferon-induced protein with tetratricopeptide repeats 1
<b>IFN</b>	Interferon
<b>IFNAR</b>	Interferon $\alpha/\beta$ receptor
<b>IL</b>	Interleukin
<b>IRF</b>	Interferon regulatory factor
<b>ISG</b>	Interferon-stimulated gene
<b>L-Particles</b>	Light Particles
<b>MCP-1</b>	Monocyte chemoattractant protein 1
<b>MHC-1</b>	Major histocompatibility complex class 1
<b>MOI</b>	Multiplicity of infection
<b>NK</b>	Natural killer
<b>OV</b>	Oncolytic virus
<b>PAMP</b>	Pathogen-associated molecular pattern
<b>PD-1</b>	Programmed death-1
<b>PFU</b>	Plaque-forming units
<b>STING</b>	Stimulator of interferon genes
<b>T-VEC</b>	Talimogene laherparepvec
<b>TGF-<math>\beta</math></b>	Transforming growth factor beta
<b>TK</b>	Thymidine kinase
<b>TLR</b>	Toll-like receptor
<b>TME</b>	Tumour microenvironment
<b>TNF</b>	Tumour necrosis factor
<b>Treg</b>	T-regulatory
<b>UV</b>	Ultraviolet
<b>WT</b>	Wild-type

## **Lay Abstract**

Cancer-killing (oncolytic) viruses (OVs) are promising new cancer treatments where a virus can target cancer cells and leave healthy cells unharmed. While OVs partially work by multiplying within cancer cells (replication), they also trigger the immune system to attack the cancer. Our lab and others have suggested that the immune-stimulating capacity of an OV is just as, if not more, important than an OV's ability to replicate. Our lab's OV is called Bovine herpesvirus type-1 (BHV-1). This project demonstrated that inactivated BHV-1 (replication-deficient) can still treat the tumours of mice just as well as its replication-competent counterpart. Analyzing the genetic profile of treated tumours suggests that both replicating and non-replicating BHV-1 have similar anti-cancer mechanisms. We also describe the immune cells that are recruited to the tumour when BHV-1 is introduced. By studying BHV-1's mechanism, we get closer to maximizing its safety and efficacy as a clinical therapy.

## **1. Introduction**

### **1.1 Oncolytic viruses**

Oncolytic viruses (OVs) are a promising approach for cancer treatment where viruses are used to selectively infect and kill cancer cells, but not healthy cells, and in many cases induce lasting systemic immunity against the cancer. The history of OVs can be traced back to anecdotes of physicians observing reduced cancer burden in patients who recovered from transmissible illnesses. One of the first examples was in 1890 when a leukemic patient had a reduction of cancerous cells following a “flu-like” infection.<sup>1</sup> Since the 1950s, we have had clinical trials exploring the use of OVs as clinical therapies ranging from RNA viruses like Newcastle disease and West Nile, to DNA viruses like adenovirus and vaccinia.<sup>1</sup> Interestingly, even the devastating SARS-CoV-2 virus that has taken millions of lives has been reported in rare cases to be associated with the regression of different cancers.<sup>2</sup> Some of the earliest trials using human viruses, however, had mixed results, and patients receiving live wild-type mumps virus, Hepatitis B virus and adenovirus still suffered from illness and side effects.<sup>3</sup>

The cancer cell-specific targeting of OVs has typically been a result of differences in the cancer cells’ cellular signaling compared to normal cells, or due to their defective anti-viral immune responses.<sup>4</sup> However, while using wild-type viruses as OVs has had modest returns, the inception of genetic engineering has propelled the field into a new era of breakthroughs in cancer virotherapy. Most importantly, genetic engineering was necessary to impart tumour cell specificity and minimize disease in human OVs, while for non-human viruses engineering would not necessarily be needed. Historically, DNA viruses have been preferentially used for genetic engineering because we have a stronger understanding of their biology and molecular

mechanisms.<sup>5</sup> Further, their relatively larger genomes allow for more flexibility and options when it comes to designing the type of genetic modification to employ.<sup>5</sup> The first instance of genetically engineering an OV was removing the thymidine kinase (TK) gene from the double-stranded DNA herpes simplex virus-1 (HSV-1), which removed its virulence in healthy cells but still allowed it to inhibit the growth of human glioma xenografts.<sup>6</sup> Other genetic modifications include the alteration of capsid structure to improve tumour tropism, insertion of tumour-specific promoters to limit replication outside cancer cells, and the addition of immune-stimulatory transgenes like cytokines to enhance the anti-tumour immune response.<sup>7</sup> To date, 5 oncolytic viruses have been approved around the world: Piconavirus-based Rigvir in Latvia, Armenia, and Georgia that targets melanoma; adenovirus-5-based Oncorine in China that targets head and neck cancers; HSV-1-based T-VEC in the US, Israel, Australia and Europe that targets metastatic melanoma; HSV-1-based Delytact in Japan that targets primary brain cancer and malignant glioma; and most recently adenovirus-based Adstiladrin in the US that targets BCG-unresponsive non-muscle invasive bladder cancer.<sup>8</sup> These milestones of approved OV therapies underscore their assured efficacy as novel cancer therapeutics, emphasizing the importance of continuing to study and develop new ones.

Historically, these therapies have been called “oncolytic viruses”. As described throughout this thesis, however, the mechanism of these viruses is not limited to their ability to induce “lysis” of cancer cells. Adstiladrin, for example, is considered a gene therapy by its manufacturer rather than an oncolytic virus because it does not replicate. While this general “oncolytic virus” nomenclature will be used interchangeably with “viral immunotherapy” throughout this thesis, it is important to recognize these caveats.

## 1.2 The role of the immune response in oncolytic virotherapy

### 1.2.1 Cellular sensing of viruses

Type I Interferons (IFN-I), namely IFN $\alpha$  and IFN $\beta$ , are primarily recognized for their capacity to trigger an antiviral state in cells, whether the cell itself is infected by a virus, or if the cell is in proximity to a virally-infected cell. This triggering initiates a program of gene transcription that disrupts multiple stages of the viral replication cycle through different mechanisms.<sup>9</sup> Nearly every cell in the body can produce IFN-I, which is typically in response to the activation of pattern recognition receptors (PRRs) by microbial components. These receptors are found on cell surfaces, in the cytosol, or within endosomal compartments, and they detect foreign nucleic acids along with a few other non-nucleic-acid pathogen-associated molecular patterns (PAMPs).<sup>10</sup> Toll-like receptors (TLR), which are a type of PRR found on cell surfaces or endosomal membranes, lead to the activation and phosphorylation of interferon regulatory factors (IRFs) like IRF3 and IRF7.<sup>11</sup> Aside from TLRs, cytosolic PRRs like retinoic acid-inducible gene-I (RIG-I) and melanoma differentiation-associated protein 5 (MDA5) that sense intracellular RNA can also lead to the activation of IRF3 and IRF7.<sup>12</sup> Similarly, cytosolic double-stranded DNA sensing is accomplished by cGAS, which upon synthesizing cyclic GMP leads to the phosphorylation of STING that also leads to the phosphorylation of IRF3.<sup>13</sup> Finally, IRF3 is a transcription factor that induces the transcription of IFN-I. IFN-I can act through autocrine, paracrine, and endocrine mechanisms by binding to IFN- $\alpha/\beta$  receptors (IFNAR) on nearly all cell types.<sup>13</sup> These receptors activate the JAK-STAT signalling pathway whereby IFN binding to IFNAR leads to phosphorylation of Janus kinases (JAKs). JAKs ultimately causes the formation the IFN-stimulates gene factor 3 (ISGF3) complex consisting of IRF9 and phosphorylated signal



transducer and activator of transcription-1 (STAT1) and STAT2.<sup>13</sup> The ISGF3 complex and IRF3 on their own can both act as transcription factors for IFN-stimulated genes (ISGs).<sup>14</sup>

In the context of a viral infection, ISGs perform a variety of functions, from prohibiting viral entry into cells and stopping viral replication, to being chemokines and chemokine receptors that attract immune cells to destroy infected cells.<sup>13</sup> While most replicating viruses can suppress the IFN signalling in some way, many can elicit stronger IFN responses without replicating and expressing viral genes that suppress immune signalling.<sup>15-17</sup> We and others have shown that enveloped viruses only need to bind and enter cells to initiate innate immune signalling within cells.<sup>15,16,18-22</sup> Our early studies revealed that non-replicating HSV-1 can induce an antiviral state within cells and induce the expression of numerous ISGs. Notably, these genes overlap with many, but not all, genes differentially regulated in response to IFN $\alpha$  on its own.<sup>15</sup> Further, we showed a diverse collection of other enveloped viruses can also induce the expression of ISGs in an IRF3-dependent, but IFN-independent mechanism.<sup>16</sup> Later, we showed that the non-structural reovirus p14 fusion-associated transmembrane protein is sufficient, on its own, to induce the expression of ISGs and generate an antiviral state in cells.<sup>21</sup> To further explore these mechanisms, we used calcium signalling as a proxy to measure membrane perturbation of cells and found that blocking calcium signalling significantly reduced an enveloped virus particle's ability to induce an antiviral state within cells, underlining the significance of a physical virus-cell interaction.<sup>23</sup> Overall, ISGs can be expressed in the absence of IFN through these signalling pathways. Thus, our lab in particular has previously used *Cxcl10*, a chemokine, and *Ifit1*, a multi-functional ISG, among a subset of ISGs as indicators of cellular

responses to incoming viruses, including inactivated virus particles.<sup>24</sup> For the present study, these two genes will be used to measure whether our cancer cells respond to incoming viruses.

### 1.2.2 The function of different immune cells

The concept that the immune system could be used against cancers dates as far back as 1890 when Dr. William B. Coley injected streptococcal organisms directly into the tumours of his patients.<sup>25</sup> While his methods were used on over a thousand patients, he came under criticism from his colleagues due to the nature of his approach. Eventually, more modern methods like chemotherapy and radiation took over as standard cancer treatments and his techniques became obsolete. As we have been re-discovering over the past many decades, however, the immune system can indeed be successfully harnessed as a powerful tool against cancer. OV's can modulate the tumour microenvironment (TME) to turn “immune cold” tumours “immune hot”, effectively reshaping the TME and providing an avenue for the induction of immunogenic cell death (ICD).<sup>26</sup> While cells may die from endogenous mechanisms such as autophagy where cells naturally degrade without stimulating the immune system, immunogenic cell death is a type of cell death that leads to the activation of an immune response by releasing signals that attract immune cells and promote inflammation.<sup>27</sup> Cancer cells in particular are often able to avoid detection by the immune system due to their defect in presenting immune-stimulatory signals that would normally elicit their destruction.<sup>26</sup> This induction of ICD by viral immunotherapies and modulation of the TME also allows tumours to better respond to immune checkpoint therapies while triggering innate and adaptive anti-tumour mechanisms within the host.<sup>28</sup>

Macrophages can have both pro-tumour and anti-tumour effects. The attraction of macrophages to the TME happens in part by the monocyte chemoattractant protein 1 (MCP-1),

also known as chemokine C-C motif ligand 2 (CCL-2).<sup>29</sup> This protein can be produced by either tumour or stromal cells within the TME, but it can also induce macrophages to produce more CCL-2 and maintain a cycle of chemotaxis.<sup>29</sup> The M1 phenotype of macrophages in particular is the phenotype that drives anti-tumour and inflammatory responses.<sup>30</sup> Other groups have shown that higher M1 macrophages within breast cancers correlate with a more favourable tumour microenvironment.<sup>31</sup> In contrast, the M2 phenotype of macrophages secretes molecules and cytokines like transforming growth factor  $\beta$  (TGF- $\beta$ ) and interleukin-10 that exert anti-inflammatory and immunosuppressive effects within the TME.<sup>32</sup> These types of macrophages have also been shown to enhance metastasis, proliferation, and angiogenesis within tumours.<sup>29</sup> Multiple OV and cancer models ranging from adenovirus for glioblastoma<sup>33</sup> to HSV-1 for breast cancer<sup>34</sup> have shown that introducing OVs into tumours leads to more macrophages acquiring the M1 phenotype. However, despite the balancing of different effects macrophages can have on tumours, clinical data overall supports the notion of high macrophage density within tumours being correlated to poor prognosis.<sup>29</sup>

Neutrophils are front-line, short-lived responders to incoming pathogens.<sup>35</sup> They have diverse roles in the context of innate immunity, including secretion of cytotoxic granules, phagocytosis, and the ability to release cytokines that recruit other immune cells.<sup>35</sup> Similar to well-characterized macrophage antitumor “M1” and protumor “M2” phenotypes, neutrophils can exhibit an antitumor “N1” phenotype, and a protumor “N2” phenotype.<sup>36</sup> In the context of OVs, studies using different models have demonstrated how they play into an OV’s therapeutic mechanism. For example, Minott and colleagues showed that systemic administration of Orf virus leads to increased circulation and infiltration of neutrophils into pulmonary melanoma

tumours.<sup>37</sup> Further, they demonstrated that neutrophils provide a significant survival advantage in tumour-bearing mice compared to their neutrophil-depleted counterparts in their model.<sup>37</sup> Our lab has also previously used neutrophil depletion to show the requirement of neutrophils in the context of a combinatorial therapy involving oncolytic HSV-1.<sup>38</sup> Overall, however, neutrophils remain relatively under-studied compared to other immune populations in the context of OV.

Dendritic cells (DCs) are antigen-presenting cells that play a crucial role in the initiation of immune responses against pathogens and cancer cells, though they are a rare immune cell population within the TME.<sup>39</sup> They capture pathogen-associated molecular patterns PAMPs and death-associated molecular patterns DAMPS from OV-infected tumours and present them to T cells, which then become activated and initiate an immune response. Type 2 CD11b+ DCs are largely associated with presenting antigens to CD4+ helper T cells, and type 1 CD103+ DCs present tumour antigens to CD8+ T cells.<sup>39,40</sup> The major indicators of dendritic cell activation are upregulated expression of MHC-1, CD40, CD80, and CD86, which have previously been measured in bone marrow-derived dendritic cells (BMDCs) from tumour-bearing mice with live and heat-inactivated vaccinia virus.<sup>41,42</sup> Aside from an OV's natural ability to stimulate DCs, groups have engineered OVs to better harness the OV's power such as encoding chemokines, cytokines, growth factors, and defensins into the viral genomes.<sup>4</sup> T-VEC in particular encodes the growth factor granulocyte-macrophage colony-stimulating factor (GM-CSF), which is known to achieve DC stimulation by inducing their maturation and attraction that enhance the priming of antigen-specific T-cells.<sup>43</sup>

Natural killer (NK) cells are lymphoid-derived innate immune cells that release perforin and granzymes to destroy virally infected cells. In the context of OV immunotherapies, NK cells have been shown to be key players in executing anti-tumour functions.<sup>44-46</sup> The mechanism for this effect is through the OV's ability to up- or down-regulate cellular stimulatory signals within cancer cells. DNAM-1 and NKG2D in particular are the major receptors on NK cells that lead to their activation, largely through recognition of CD155 and CD112 on tumour and virally-infected cells.<sup>47</sup> Inhibition of NK cells comes from their recognition of self-HLA class 1. This molecule is widely present on normal cells, but down-regulated in tumours and virally-infected cells.<sup>47</sup> NK cells can also be characterized by their activated state with a CD69 marker,<sup>48</sup> and cytotoxic state with Granzyme B.<sup>49</sup> A variety of OVs based on viruses like adenovirus, measles, Newcastle disease virus, and HSV-1 have been shown to increase the infiltration of NK cells into the tumour.<sup>50</sup> Further, studies depleting NK cells from animal models have shown decreased efficacy of OVs, which underscores the crucial role NK cells can play in OV therapy for their cytotoxic effects and cytokine production.<sup>44-46,50</sup>

B cells are an essential part of the adaptive immune system and are responsible for the production of antibodies against foreign pathogens. When a B cell encounters a foreign antigen, it differentiates into either an antibody-producing plasma cell, or a memory B cell that “remembers” the antigen and can generate antibodies rapidly the next time the antigen is encountered.<sup>51</sup> In the context of OV immunotherapies, B cells have been shown to be critical for the mechanisms of these therapies. For example, our lab has previously conducted a B-cell depletion study on mice treated with a combination therapy using oncolytic HSV-1 and found that depletion of B cells abolishes the survival benefit of the therapeutic regimen.<sup>52</sup> Another

group harvested serum from mice previously treated with their oncolytic HSV-1 platform and administered that serum into mice bearing tumours that had never received OV administration. They found that the serum alone from treated mice was effective at significantly reducing the size of tumours in these naïve mice.<sup>53</sup> The same group validated this effect across three different cancer models: hepatoma (Hepa 1-6 cells), renal (Renca cells), and B cell lymphoma (A20), which shows how broadly applicable the effect of B cells on viral immunotherapies can be. More importantly, the study shows how viral immunotherapies can cause the host to generate antibodies against tumours, not just against the virus, regardless of tumour model.

CD8<sup>+</sup> T cells play a critical role in the adaptive immune response. CD8<sup>+</sup> T cells in particular are responsible for recognizing and killing cells that have been infected with viruses or have become cancerous. In cancer immunotherapy, CD8<sup>+</sup> T cells are the most powerful effectors in the anticancer immune response and form the backbone of current successful cancer immunotherapies.<sup>54</sup> Their activation happens by detection of tumour-related antigens to kill tumour cells, which largely determines the antitumor effect.<sup>55</sup> However, this activation towards an anti-tumour state also requires interaction with DCs. Notably, the production of interleukin-12 by DCs within the tumour is critical for the stimulation and proliferation of cytotoxic CD8<sup>+</sup> T-cells.<sup>56,57</sup> When stimulated, cytotoxic CD8<sup>+</sup> T cells can exert their anti-tumour effects through various pathways. These mechanisms include releasing cytokines like IFN $\gamma$  and tumor necrosis factor (TNF), engaging death receptors such as FAS and TRAIL, targeting tumour vasculature, and deploying granule-associated enzymes like perforin and granzymes through granule exocytosis.<sup>58</sup> Interestingly, not all modes of effector functions are necessarily engaged or required for effective tumour control, as the impact of specific effector or cytotoxic pathway

deficiencies can vary across different mouse models.<sup>58</sup> However, CD8<sup>+</sup> T cells within tumours are not always stimulated and attacking tumours. Indeed, CD8<sup>+</sup> T cells can become “exhausted”, a state where their function deteriorates if they are chronically exposed to stimulatory signals.<sup>59</sup> This state can be characterized by the expression of multiple inhibitory receptors like PD1, LAG3, CTLA4, and TIM3. The exhaustion ultimately leads to failure in producing cytokines such as IFN $\gamma$  and TNF, as well as cytotoxic molecules including granzymes and perforin. Many of the most commonly studied OVs based on viruses like HSV-1, vaccinia, and adenovirus have been shown to increase infiltration of CD8<sup>+</sup> T cells into tumours and exert cytotoxic effects.<sup>60</sup> Further, immune checkpoint inhibitors, as discussed later, have been successfully used in combination with OV therapy because they can also further increase the infiltration of CD8<sup>+</sup> T cells into tumours or reduce their exhaustion.<sup>60</sup>

CD4<sup>+</sup> T cells are the supportive allies to other immune cells, including their CD8<sup>+</sup> counterparts. They can support tumour effects of CD8<sup>+</sup> by secreting cytokines such as interleukin-2 (IL-2), which binds to the IL-2 receptor on CD8<sup>+</sup> and lead to their proliferation and activation of effector functions.<sup>61</sup> CD4<sup>+</sup> T cells can also express the CD154 ligand, which binds to CD40 receptors on DCs and leads to the DCs further activating the cytolytic capacity of CD8<sup>+</sup> T cells.<sup>62</sup> Similar to CD8<sup>+</sup> T cells, CD4<sup>+</sup> T cells can also exhibit direct toxicity and cytolytic activity against tumour cells, though this is rare.<sup>63</sup> A distinct population of CD4<sup>+</sup> are the T-regulatory (Treg) cells, which have been repeatedly found to exert pro-tumour effects through mechanisms like secreting immune-suppressive cytokines like interleukin-10 and transforming growth factor- $\beta$  into the TME.<sup>61</sup> Tregs are defined by the presence of CD25 on their surface, and their activation is marked by the transcription factor FoxP3.<sup>64</sup> In our lab, we have found that our

model oncolytic virus, Bovine herpesvirus type-1 (BHV-1) can reduce the infiltration of suppressive Tregs in the context of a therapeutic regimen.<sup>65</sup> In the clinic, the approved G47 $\Delta$  HSV-based OV in Japan has been found to increase the number of CD4<sup>+</sup>/CD8<sup>+</sup> lymphocytes in tumour biopsies, while FoxP3<sup>+</sup> cells remain low.<sup>66</sup> Ultimately, CD4<sup>+</sup> T cells appear to have either anti- or pro-tumour effects depending on their particular subtype.



### 1.3 Combination therapies

While viral immunotherapy is a promising anti-cancer strategy, these viruses often need to be used in combination with other cancer therapies. One group reviewed how the combination of different immune-stimulatory signals from cells induced by diverse treatments can be required for immunogenic cell death, hence why combining OV<sub>s</sub> with different treatments is sometimes required for efficacy.<sup>26</sup> Generally, receptors on cells can either activate cell signaling pathways by recruiting kinases that cause phosphorylation, or inhibit cell signaling by recruiting phosphatases that cause dephosphorylation.<sup>67</sup> Immune checkpoints are naturally occurring cellular molecules that normal cells, cancer cells, and even antigen presenting cells can use to “turn off” signaling pathways of different immune cells and inhibit their activity.<sup>68</sup> Immune checkpoint receptors include ones like TIM-3 expressed on CD4<sup>+</sup> T cells that binds galectin-9, SIRP $\alpha$  on macrophages that binds CD47, LAG-3 on Treg cells that binds to MHC II, and PD-L1 on different T cells that binds to PD-1.<sup>68,69</sup> In the context of cancer, tumours can exploit these inhibitors by expressing them on their surface to prevent attack by the immune system. The utilization of immune checkpoint inhibitors (ICIs) in treating different cancers has garnered approval from the US Food and Drug Administration (FDA). Initially, in 2011, ipilimumab (anti-cytotoxic T-lymphocyte associated protein 4 [CTLA4]) gained FDA approval for metastatic melanoma treatment, followed by other checkpoint inhibitors targeting the PD-1/PD-L1 axis for several tumor types.<sup>70</sup> Despite initial positive responses, patients treated with immune checkpoint inhibitors often develop resistance over time, leading to recurrences.<sup>71</sup> Consequently, combination therapies, involving the simultaneous administration of immune checkpoint inhibitors and other anticancer agents such as OV<sub>s</sub>, continue to be studied. More specifically, OV<sub>s</sub> and ICIs work synergistically through different mechanisms. OV<sub>s</sub> trigger inflammation

within the TME, which primes the TME for enhanced immune cell infiltration.<sup>60</sup> Subsequently, ICIs further potentiate this response by blocking these inhibitory checkpoints, allowing activated immune cells to exert their anti-tumour effects more effectively, resulting in a combined therapeutic approach that enhances anti-tumour immunity.<sup>60</sup> So far, OV<sub>s</sub> based on adenovirus, HSV-1, and vaccinia virus have been combined in the clinic with PD-1, PD-L1, and/or CTLA-4 ICIs to varying degrees of efficacy.<sup>60</sup>

Chemotherapy drugs can also be combined with OV<sub>s</sub>, which can result in enhancing OV cytotoxicity or reducing the immunosuppression caused by the tumour. Fludarabine<sup>72</sup> and paclitaxel<sup>73</sup> are examples of chemotherapy agents that have been shown to reduce T regulatory cells in cancer patients, which as discussed earlier are a cell population that contributes to immunosuppression. Myeloid-derived suppressor cells (MDSCs), which are a heterogeneous group of immune cells typically protective in healthy tissues, can foster tumour growth by hindering antitumor responses in the tumour environment.<sup>74</sup> One study found that intratumoral injection of an HSV-1-based OV following injection of the drug gemcitabine reduces MDSCs and enhances their vector's oncolytic activity.<sup>75</sup> Similarly, another study showed that mean tumour volumes of mice treated with Sendai virus particles combined with the chemotherapy drug sunitinib reduced mean tumour volumes more than virus alone in a regression experiment.<sup>76</sup> In our lab, we have consistently shown beneficial outcomes in mouse tumour models when combining our viral immunotherapies with low/non-cytotoxic dose of chemotherapeutics like the FEC cocktail (5-fluorouracil, epirubicin, cyclophosphamide),<sup>77</sup> mitoxantrone,<sup>38</sup> and Mitomycin C.<sup>30,65,78</sup> Overall, however, a meta-analysis comparing the efficacy of OV<sub>s</sub> combined with chemotherapy agents versus OV<sub>s</sub> combined with ICIs concluded that the ICI+OV combination had overall better efficacy than the chemotherapy + OV combination.<sup>79</sup>

## 1.4 Bovine herpesvirus type-1

Bovine herpesvirus type-1 (BHV-1) is an alphaherpesvirus that causes a variety of ailments in cattle. These include conjunctivitis, upper respiratory tract disorders, abortions, and transient immune suppression.<sup>80</sup> BHV-1 can also replicate in and kill numerous human immortalized and cancerous cell lines, but not healthy cells. One advantage of BHV-1 as an immunotherapy is that it has a strict host range, with no human disease or seroconversion having been detected in humans.<sup>81</sup> Further, BHV-1 has been found to target both bulk and tumour-initiating cells irrespective of their receptors or mutations.<sup>81,82</sup> In a study screening the effects of BHV-1 on the NCI60 panel of established human tumour cell lines, 72% of cell lines had a decrease in cellular viability in response to BHV-1 infection.<sup>83</sup> This result is compared to a sensitivity of only 32% for the oncolytic herpes simplex virus 1 (oHSV-1)-based oncolytic vector tested in the study.<sup>83</sup> Of note, however, 35% of the panel showed minimal to no BHV-1 replication, yet still had decreases in cellular viability, which brings into question how and when replication is required for BHV-1's anti-tumour efficacy.<sup>83</sup> Though BHV-1's therapeutic mechanism is still largely unknown, the study also revealed that KRAS mutations, and not IFN signalling, appear to correlate with high levels of BHV-1 replication.<sup>83</sup> In lung adenocarcinoma cells, BHV-1 also reduces the levels of histone deacetylases,<sup>84</sup> which the FDA has approved as drug targets to treat a variety of cancers.<sup>85</sup> Our lab has also recently published a study showing BHV-1's efficacy in the context of a therapeutic regimen within an *in vivo* model.<sup>65</sup> In that study, we showed that combining BHV-1 with the chemotherapy drug Mitomycin C and immune checkpoint inhibitors against PD-1 and CTLA-4 significantly extends the survival of tumour-bearing mice in our syngeneic melanoma model. Further, this therapy can induce immunogenic cell death as well as activate circulating CD8<sup>+</sup> T cells and reduce the tumour infiltration of T

regulatory cells. Lastly, the *in vivo* transcriptome analysis of Live BHV-1-treated tumours previously found that mitomycin causes an upregulation of genes involved in myeloid cell regulation and other myeloid-pathway-related genes.<sup>65</sup> For this reason, it would be of interest to analyse the infiltration of neutrophils and macrophages, both of which have previously been implicated in viral immunotherapies by our and other groups.<sup>30,37,38,77,86-88</sup> While there is much we have learned about BHV-1 and its mechanism, one outstanding question is whether it needs to replicate in order to be an effective therapeutic.

### **1.5 Is viral replication needed for an OV to be effective?**

Traditionally, the replication potential of an OV has been correlated to its therapeutic efficacy. For example, one study used small molecules to increase the replication of their oncolytic HSV-1 vector, which led to enhanced and synergistic anti-tumour activity *in vivo*.<sup>89</sup> Another study used a small molecule to block cellular pathways associated with cytosolic DNA sensing. The molecule was found to augment the replication of their oncolytic vaccinia virus and promote cell death of their ovarian cancer cell line.<sup>90</sup> This study, however, did not test the efficacy of this drug *in vivo*. One group found that adenovirus with a modified early protein E1A engineered to overexpress the adenovirus death protein (ADP) demonstrated heightened replication and spread in human A549 lung carcinoma cells, resulting in decreased tumour size in A549 tumours implanted in nude mice compared to the parental virus strain.<sup>91</sup> As the anti-viral effect of the immune system has been thought of as a barrier to OV replication and spread, some studies have also focused on, and had success with, combining OVs such as poxvirus<sup>92</sup> and HSV-1<sup>93</sup> with immunosuppressants. As described earlier, however, although the selective replication of OVs within tumour cells has conventionally been credited for their tumour-killing effects, the induction of host antitumor immunity also plays a significant unambiguous role.<sup>94,95</sup>

Therefore, it is possible that viral immunotherapies need to activate the immune system to a degree that stimulates a strong anti-tumour response, but a weak or absent anti-viral response.

As described earlier, we and others have previously shown that binding and penetration of enveloped virus particles are sufficient to trigger innate immune signalling; viral replication is not necessarily required.<sup>21-24</sup> Previous data from our lab shows that a mutated HSV-1 vector with lower replication *in vitro* still exhibits strong oncolytic activity *in vivo*.<sup>96</sup> In the aforementioned study using the NCI60 panel comparing BHV-1 and HSV-1, significant decreases in cellular viability still occurred in cells that did not support BHV-1 replication.<sup>83</sup> More recently, we have found that the chemotherapy drug mitomycin C—which inhibits BHV-1 replication—improves the efficacy of BHV-1 *in vivo*, suggesting that replication might hinder BHV-1's therapeutic potential.<sup>65</sup>

In the broader context of immunotherapy, one study showed that heat-inactivated (HI) and UV-inactivated (UV) vaccinia virus were able to induce significantly higher expression of different interferons and innate immune cytokines in murine melanoma and dendritic cells.<sup>42</sup> The same study showed that HI and UV vaccinia conferred significant survival benefits in mice challenged with B16-F10 melanoma tumours compared to PBS.<sup>42</sup> Another study found that their heat-inactivated vaccinia models induced cytokines, IFN-1, and chemokines in DCs while their replicating vaccinia did not.<sup>41</sup> The same study also found that heat-inactivated vaccinia was more effective at eradicating tumours than its replicating counterpart.<sup>41</sup> Another study used UV HSV to stimulate human NK cells *in vitro* and showed a survival benefit in a xenograft mouse model of human acute myeloid leukemia that received administration of these stimulated NK cells.<sup>97</sup> A

follow-up study by the same group showed that UV HSV can also stimulate NK cells to lyse prostate cancer cells *in vitro*.<sup>98</sup> Further, the dependency of an OV's efficacy on innate immune signalling is underscored by a group that treated WT and STING-KO tumours with oncolytic HSV-1 and found that the STING-KO tumours were more resistant to their treatment regimen than STING-WT tumours.<sup>99</sup> In our own lab, we have also previously witnessed an inverse correlation between the replication of an OV *in vitro* and its efficacy *in vivo*.<sup>96</sup>

Taken together, these data suggest that the anti-tumour effects of large DNA enveloped viruses could be augmented, or at least maintained, by impairing their ability to replicate. Thus, given the well-documented role of the immune system in viral immunotherapies,<sup>94</sup> it is possible that non-replicating BHV-1 could be just as, if not more, effective at prolonging survival of mice with tumours than live BHV-1. Such viral particles would also have an improved safety profile for patients as this approach would limit the administration of live biological agents.

Alternatively, however, the lack of replication would result in less production of new viral particles and viral PAMPs that could theoretically augment the anti-tumour immune response. Viral immunotherapy relies on a balance between a virus' ability to stimulate or suppress an immune response. Thus, it would be valuable to investigate whether inactivating BHV-1 tilts this balance in a way that improves, worsens, or maintains its *in vivo* therapeutic efficacy.

## 1.6 UV inactivation

Different models can be used to test the efficacy of non-replicating herpesvirus particles, namely: (1) heat inactivation, (2) Light particles (L-particles), and (3) inactivation by UV radiation. Heat can be used to inactivate viral particles by denaturing the secondary structure of proteins, which can impair their ability to bind and enter cells.<sup>100</sup> In addition to infectious virions, an  $\alpha$ -herpesvirus infection will also produce L-particles during replication.<sup>101</sup> These particles have an envelope and tegument proteins, but do not have capsids or genomes and thus are unable to replicate.<sup>101</sup> In a typical BHV-1 preparation, up to half of the extracellular particles can be L-particles.<sup>102</sup> Given their conserved envelope, these particles could still have the ability to bind and enter cells, which could make them immunostimulatory on their own. UV radiation inactivates particles by directly cross-linking DNA to form pyrimidine dimers, which can interfere with viral DNA replication and viral mRNA production.<sup>103</sup> To a lesser extent, UV radiation can also target chromophores on proteins, namely the aromatic side chains of tyrosine, tryptophan, phenylalanine, and disulfide cystine bonds.<sup>104</sup> Studies that use UV-inactivated viruses for their experiments do not always discuss the nuances of their UV-inactivation method. Namely, they do not usually specify the light source or wavelength that was used, and these differences make it difficult to compare UV conditions from one paper, or one virus, to another. UV rays are classified into subspectra, specifically UVA (320–400 nm), UVB (280–320 nm), and UVC (< 280 nm). UV mercury lamps only radiate a single or broad range of wavelengths simultaneously, whereas their LED counterparts can be modified to radiate UV at any point of the UV spectra. Interestingly, a study comparing the efficacy of mercury lamps and UV-LEDs at reducing influenza (another enveloped virus) titers showed that a 254nm treatment of 4.8mJ/cm<sup>2</sup> from a mercury lamp reduced viral titers by the same amount as a 280nm treatment of the same

energy by a UV-LED.<sup>105</sup> While other methods of inactivating viruses such as formalin, psoralen, and genetic alterations are possible avenues to study an inactivated virus, UV is a method our lab has experience with and showed promising characteristics in preliminary experiments.

## 1.7 Study objectives and hypothesis

While in our lab we have consistently observed a negative correlation between replication capacity and anti-tumour activity, we have never definitively tested whether replication is necessary for a viral immunotherapy. *For my project, I hypothesized that replication-**incompetent BHV-1 will retain its anti-cancer efficacy in vivo.*** To achieve this, it is necessary to optimize conditions that allow for BHV-1 to be inactivated without eliminating its ability to be sensed by our cancer cell line, which can be evaluated by measuring ISG expression of these cancer cells infected with inactivated BHV-1. Upon optimizing these conditions, we can measure whether BHV-1 extends the survival of tumour-bearing mice, analyze the transcriptome of these tumours, and explore which immune cell populations infiltrate the tumour upon treatment with either kind of virus. By analyzing the transcriptome of tumours and the cells the tumours derive from in response to BHV-1 infection, we can begin developing a framework for protocols that could help us screen new BHV-1 mutants *in vitro* before testing their efficacy *in vivo*. Thus, this thesis will present three major aims of the research conducted:

1. To optimize a viable non-replicating BHV-1 platform.
2. To evaluate whether inactivated BHV-1 is as effective as live BHV-1 at extending the survival of tumour-bearing mice.
3. To analyze the transcriptome and immune-cell infiltration profile of BHV-1-treated tumours to better understand its mechanism.



## **1.8 Implications of this study**

Recent findings within the field of OV's are reshaping the central dogma that replication is correlated to efficacy. While several animal models have demonstrated the efficacy of inactivated viruses in recent decades, clinical data are now also beginning to show that this notion could extend to humans. BHV-1 has shown potential as an immunotherapy in our lab's animal model, and we hope to one day bring it to clinical trials. The aims of my thesis will help us understand more about BHV-1's biology as an immunotherapy and the minimal requirements for its efficacy. This thesis will also add to the growing body of literature trying to answer the same question on everybody's mind: do oncolytic viruses truly need to replicate?

## **2 Materials and Methods**

### **2.2 Cells**

CRIB cells,<sup>106</sup> derived from Madin-Darby bovine kidney (MDBK) cells to be resistant to Bovine Viral Diarrhea Virus (BVDV) and other pestiviruses,<sup>107</sup> were generously gifted by Dr. Clinton Jones (Oklahoma State University, US) and cultured in Dulbecco's modified Eagle's medium (DMEM) supplemented with 5% fetal bovine serum (FBS) and 1% L-glutamine. C10 cells<sup>108</sup> (derived from B16 B78H1 mouse melanoma cells) expressing human Nectin-1 were generously gifted from Dr. Gary Cohen (University of Pennsylvania, US) and maintained in DMEM supplemented with 5% FBS, 100 U/mL penicillin–streptomycin and 250 µg/mL Geneticin (Gibco Cat# 10131035). C10 cells express human Nectin-1.

### **2.2 Viruses**

BHVgfp,<sup>109</sup> the BHV-1 mutant used for all experiments except those in Figure 5, was generously gifted by Dr. Günther Keil (Friedrich-Loeffler-Institut, Greifswald, Mecklenburg-Vorpommern, Germany) and has a partial deletion in the gI locus. Figure 5 was produced using BHVgIgE, which is a BHV-1 mutant created in our lab to have full deletions of the gI and gE loci. Both virus mutants have an insertion of enhanced green fluorescent protein (GFP) controlled by a murine cytomegalovirus (CMV) promoter. CRIB cells were used to propagate and titer both viruses. Preparations involved sucrose cushion purification, and the purified virus was resuspended in PBS + 10% glycerol and stored at -80°C.<sup>82</sup> Any reference to “BHV-1” throughout the text is BHVgfp unless otherwise stated.

### **2.3 Plaque assays**

Confluent CRIB cells on 12-well plates were infected with serial dilutions of BHV-1 in 250 $\mu$ L. Inoculation was carried out at 37°C for 1 hour with rocking every 10-15 minutes. Cells were washed with PBS and overlaid with DMEM + 1% methylcellulose, 1% FBS, and 1% L-glutamine. Viral titres were measured after 3 days by counting plaques following GFP scanning.

## **2.4 Growth curves**

CRIB and C10 cells were infected with a multiplicity of infection (MOI) of 0.1 of either live or UV BHV-1 in triplicate, and crude lysate (cells + supernatant) was collected every 24 hours for 5 days. The crude lysate was freeze-thaw-vortexed 3 times and spun down. The supernatant was used to perform a plaque assay that measured the virus produced over 5 days by either live or UV BHV-1.

## **2.5 Optimizing conditions for heat inactivation**

BHV-1 aliquots (100 $\mu$ L each) from the same stock were diluted 1:10 with PBS, put into water baths at either 37°C, 55°C, or 70°C, or into a thermocycler at 56°C for varying times. After heat treatment, a plaque assay was run using permissive CRIB cells to determine titer. A sample of BHV-1 was defined to be “heat-inactivated” when no plaques could be observed following a plaque assay.

## **2.6 Optimizing conditions for UV inactivation**

UV inactivation was defined to be the condition needed to reduce viral titers a minimum of 10<sup>5</sup>-fold as done previously by our lab.<sup>16</sup> UV inactivation of BHV-1 was performed using a mercury lamp ultraviolet crosslinker emitting 254nm UV-C radiation (Stratalinker). To

determine the amount of UV radiation needed to inactivate BHV-1, a virus stock was diluted to  $3 \times 10^6$  PFU/mL for optimizing conditions for *in vitro* experiments, and  $4 \times 10^8$  PFU/mL for optimizing conditions for *in vivo* experiments. Diluted virus was put into the UV cross-linker and treated with energies varying from 100-700mJ/cm<sup>2</sup>. Immediately following UV treatment, a plaque assay was run using permissive CRIB cells to determine what condition met the definition of UV inactivation. To verify inactivation using  $4 \times 10^8$  PFU/mL, a growth curve was also performed.

## 2.7 Quantitative RT-PCR

Mouse melanoma C10 cells were mock-infected or infected with an MOI of 10 of live, UV, or heat-inactivated BHVgfp or BHVgIgE depending on the experiment, unless otherwise indicated. RNA was harvested at indicated time points after infection using the RNeasy Plus Mini Kit (Qiagen Cat# 74136). The iScript™ gDNA Clear cDNA Synthesis Kit (Bio-Rad Cat# 1725034) was used to synthesize cDNA. qRT-PCR was performed in triplicate using *Ifit1* (Thermofisher Cat# 4331182, Mm00515153\_m1), and *Cxcl10* (Thermofisher Cat# 4351368, Mm00445235\_m1) TaqMan primer/probes to measure gene expression with the qPCR Fast Advanced TaqMan Master Mix (Thermofisher Cat# 4444556). Eukaryotic 18S rRNA (Thermofisher Cat# 4319413E) was used to normalize gene expression.

## 2.8 Transcriptome profiling

For the *in vitro* transcriptome analysis, melanoma C10 cells were mock-infected or infected with live or UV BHVgfp, either in the presence of 20µg/mL Mitomycin C (Sigma Cat# M5353) or DMSO (vehicle control) and RNA was harvested at 6 and 12 hours post infection (hpi). The microarray that was used is the ThermoFisher Affymetrix Clariom S Mouse Assay (Cat. # 902930), which provides a transcriptome-wide analysis of over 20,000 annotated genes. In summary, 12 groups were analyzed using the Clariom S Mouse Assay: C10 cells infected with live, UV BHV-1, and mock-infected—each with or without mitomycin, at 6hpi and 12hpi. This process was repeated 3 times to generate 3 biological replicates, totalling 36 samples.

For *in vivo* transcriptome analysis, C10 tumours were treated with either PBS or UV BHV-1 +/- Mitomycin C (Sigma Cat# M4287). Transcriptome data from tumours treated with live BHV-1 was taken from our lab's previous study.<sup>65</sup> Tumours were harvested 5 days post-treatment and homogenized in Trizol Reagent (Thermo Cat# 15-596-018). Following homogenization, chloroform was added and samples were left to incubate at room temperature for 3 minutes. Samples were centrifuged at 12,000xg for 15min at 4°C and the top aqueous layer was mixed with 70% ethanol in a separate tube. RNA from this mixture was isolated, diluted to 100ng/µL and reverse transcribed. sscDNA was purified using magnetic beads and fragmented using UDG. The fragmented samples were hybridized to the Affymetrix Clariom S Mouse Assay (Cat. # 902930), and the stained arrays were scanned to generate intensity data. All of the reagents for this assay were developed by and purchased from Thermo Fisher Scientific. Raw data were analyzed using the ThermoFisher's Transcriptome Analysis Console (TAC) software, version 4.0.2.1.5. For all analyses, only genes with a fold-change in expression >3 were included.

## **2.9 Drug and antibody preparation for *in vivo* experiments**

Mitomycin C powder (Sigma Cat# M4287) was dissolved in sterile water to a concentration of 2 mg/mL, and a new bottle was used for each experiment. Anti-mouse  $\alpha$ -CTLA-4 and  $\alpha$ -PD-L1 antibodies (BioXCell Cat# BE0131 and BE0101, respectively) were diluted to 1 mg/mL with sterile PBS.

## **2.10 Tumour regression of mice bearing C10 tumours treated with live or UV BHV-1**

The schematic for this experiment is outlined in Figure 7a and is based on a previously established therapeutic regimen<sup>65</sup>. Six- to eight-week-old C57Bl/6 female mice were implanted with  $5 \times 10^6$  C10 cells resuspended in 200  $\mu$ L PBS subcutaneously into the left flank. After ~2 weeks when tumours reached sizes between 50-100mm<sup>3</sup>, mice were treated with 100 $\mu$ g Mitomycin C or sterile water as a vehicle control intratumorally (Day 1). Every day from days 2-4, mice received intratumoral injections of  $2 \times 10^7$  PFU live BHV-1, equivalent volume of UV BHV-1, or PBS. Mice also received intraperitoneal injections of  $\alpha$ -CTLA-4 and  $\alpha$ -PD-L1 antibodies (200  $\mu$ g each) starting on day 2 and every 3 days for 10 total doses. Tumours were measured every 3-4 days and mice were considered endpoint when tumour volumes reached 550mm<sup>3</sup>. All animals were cared for by the McMaster University Central Animal Facility. Procedures were performed in full compliance with the Canadian Council on Animal Care and approved by the Animal Research Ethics Board of McMaster University.

## **2.11 Tumour infiltration of immune cells**

Tumours were harvested and minced with a razor blade in RPMI + 10% FBS. Then, 50 µg/mL liberase (Sigma Cat# 5401054001) was added for digestion and samples were incubated for 1 hour at 37 °C with constant stirring. The cell suspension was passed over a 100-micron filter and rinsed with 5 mL of RPMI + 10% FBS. Cells were pelleted and ACK Lysis buffer (Quality Biological Cat# 118-156-101) was used to lyse red blood cells. Viability staining was done using the Zombie UV Fixable Viability Kit (BioLegend Cat# 423107). Cells were treated with anti-CD16/CD32 (Fc block; BD Biosciences Cat# 553141) and surface stained with fluorescently conjugated antibodies against F4/80 (BD Biosciences Cat# 565635), Ly6G (BD Biosciences Cat# 569406), CD8 (BD Biosciences Cat# 563046), CD45 (BD Biosciences Cat# 562420), CD4 (BD Biosciences Cat# 552775), CD11b (BD Biosciences Cat# 553311), CD3 (BD Biosciences Cat# 561388), and NK1.1 (BD Biosciences Cat# 550627). Cells were then intracellularly stained with anti-FoxP3 (BD Biosciences Cat# 560403). The CytoFLEX LX flow cytometer was used for data acquisition and the FlowJo Software version 10.10.0 was used for data analysis.

## **2.12 Statistical Analysis**

A student's t-test was used to compare the means between two groups of data. Kaplan–Meier curves were used to estimate survival, and the log-rank Mantel-Cox test was used to determine the difference in survival. p-values less than 0.05 were considered significant. All data analyses were carried out using GraphPad Prism version 9.3.1.

### 3 Results

#### 3.2 Developing an inactivated Bovine herpesvirus type-1 (BHV-1) platform

##### 3.2.2 Different temperatures and durations lead to heat inactivation of BHV-1

BHV-1 stocks were heat-inactivated (HI) in a water bath or thermocycler at different temperatures and varying times to test which conditions led to inactivation, which was defined as no visible plaques following a plaque assay analysis. The water bath temperatures of 37°C, 55°C, or 70°C were selected based on previous literature with different viruses,<sup>41,110</sup> and these were the first temperatures tested. Water baths were initially used for their larger capacity and convenience, though a thermocycler was later used for its better precision in maintaining set temperatures. Heat inactivation was achieved at 55°C for 24hr and 70°C for 5min in a water bath, or 56°C for 30 minutes in a thermocycler (Figure 1). Incubating BHV-1 at 55°C yielded inconsistent results throughout the different time points where some longer incubation times resulted in higher plaque counts than shorter incubation times. This variability could be due to 55°C potentially being close to the threshold of denaturing temperature needed for proteins on BHV-1's required for binding and entering, compounded with the practical limitations of a water bath maintaining a steady temperature for a prolonged period. At 37°C, there was little observable decrease in BHV-1 titer between incubation at 0hr and 48hr. Given that BHV-1 is a virus that would be adapted to live within a bovine host whose average temperature is close to 37°C,<sup>111</sup> it makes sense that BHV-1 would retain its ability to replicate even after 48hr at 37°C. Incubating at 70°C in a water bath was the quickest, requiring at most 5 minutes for complete inactivation. Lastly, A few months following inactivation using water baths, a paper was published that used 56°C for 30 minutes to inactivate BHV-1.<sup>112</sup> Due to the variable and unreliable results from inactivation at 55°C in a water bath, a thermocycler was used to test this



new condition and avoid the temperature variations that can happen in water baths. In the present study, incubating at 56°C in a thermocycler required more than 15 minutes, but no more than 30 minutes for complete inactivation.

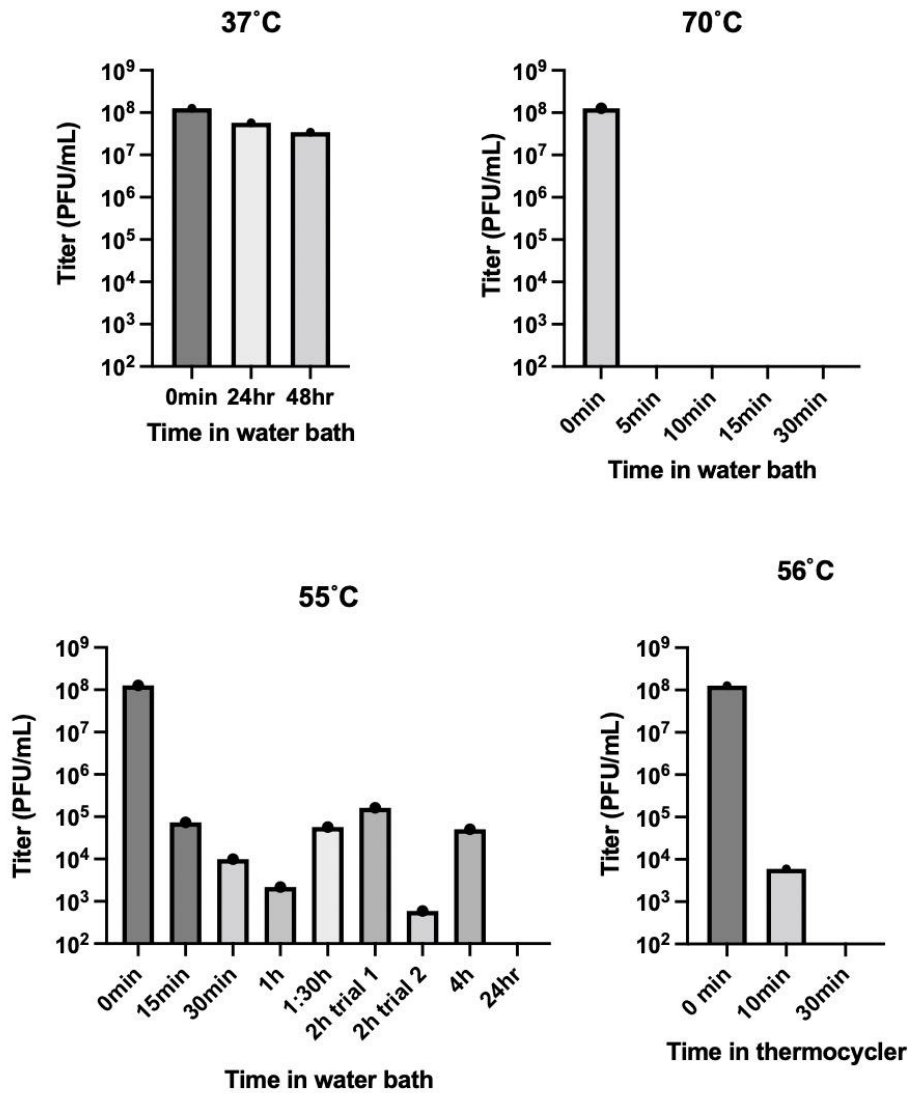


**Figure 1. Optimization of BHV-1 heat-inactivation.**

Diluted BHV-1 stocks were inactivated in either a water bath or a thermocycler. After heating, plaque assays were used to determine titer. Conditions with no visible plaques were determined to be completely heat inactivated. Each condition was tested with a single technical and biological replicate with the exception of 2h at 55°C, which was tested twice across two separate experiments (trial 1 and trial 2).

### 3.2.3 Treating BHV-1 at 70°C for 5 minutes does not affect overall virion structure

A concern with heat inactivation is that the heat could cause virions to partially denature or alter their conformation, thus it was imperative to evaluate their integrity following inactivation before further experiments could be done. For this experiment, the heat inactivation condition chosen to investigate was 70°C for 5 minutes. The Izon qViro Particle Counter is an instrument that can analyze the size and quantity distribution of particles in the nanometer size range. Live BHV-1 and BHV-1 heated to 70°C for 5 min were analyzed, and the overlapping histograms (Figure 2) suggest that overall particle integrity is conserved following heat inactivation. However, these data do not provide insight into any proteins that may have been denatured, though not enough to destroy the virion.

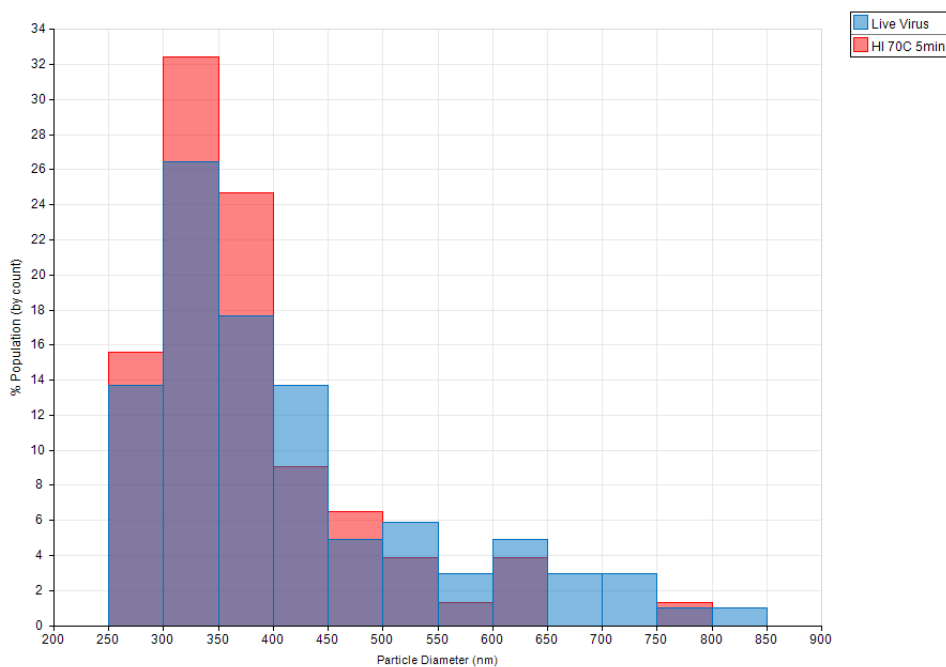


**Figure 2. Size distribution of live and oBHV-1 inactivated at 70°C for 5 min.**

Live BHV-1 particles (blue) and BHV-1 inactivated for 5 minutes at 70°C (red) were analyzed using the Izon qViro Particle Counter. Overlapping histograms suggest overall particle integrity is conserved. Graph shows the result of a single experiment.

### 3.2.4 HI BHV-1 does not induce the expression of interferon-stimulated genes (ISGs)

To determine whether HI BHV-1 could still stimulate innate immune signaling within our melanoma cancer cell model (C10), C10 cells were infected with live or HI BHV-1 at varying MOIs across different experiments and the expression of the ISGs *Ifit1* and *Cxcl10* were measured with RT-qPCR. Repeated experiments measuring the expression of these ISGs in C10 cells showed that heat inactivation abolishes BHV-1's ability to induce ISGs (Figure 3). C10 cells infected with HI BHV-1 at 70°C for 5min and/or 56°C for 30min using volumes equivalent to MOIs of 1.25, 5, 10, and 20 all lead to no observable increase in fold change compared to mock-infected cells.

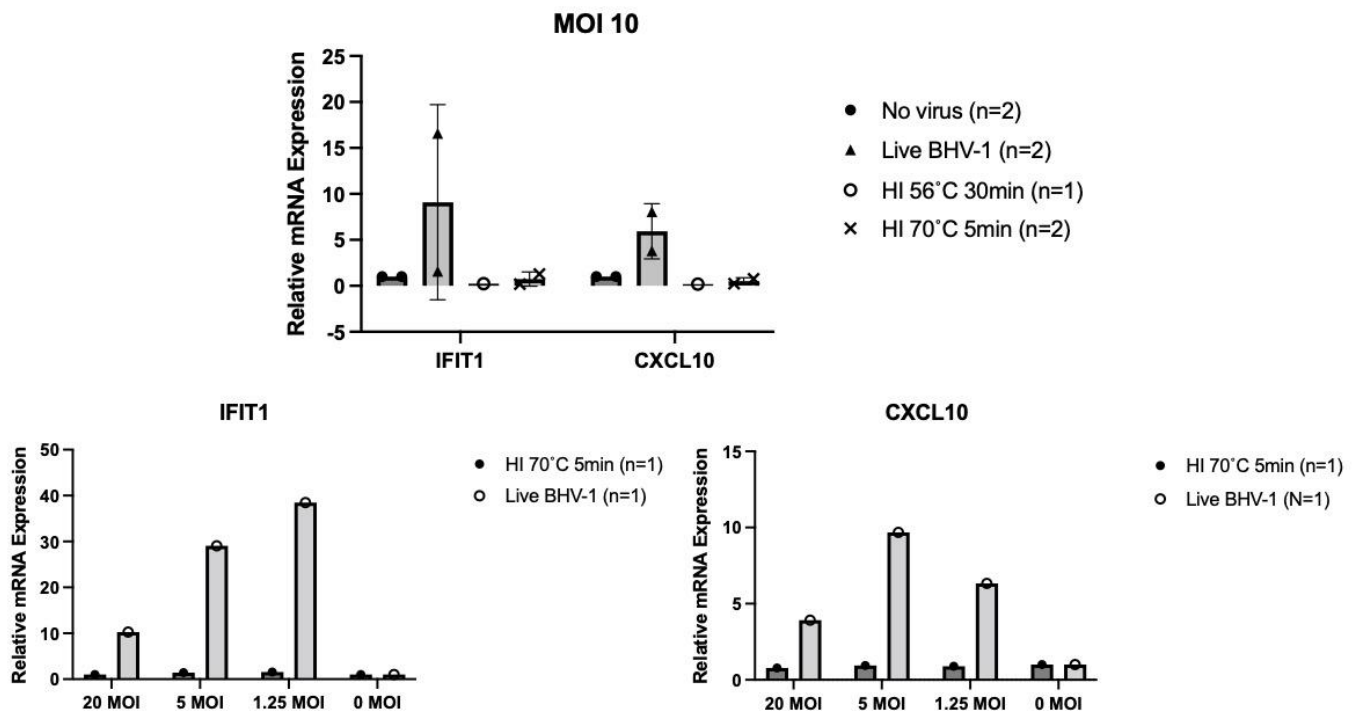


**Figure 3. Heat-inactivated BHV-1 fails to induce interferon-stimulated gene (ISG) expression in C10 cells at 6hpi.**

Mouse melanoma C10 cells were mock-treated (No virus), treated with live BHV-1, or HI BHV-1 using two different heat-inactivation conditions at different MOIs. Relative gene expression of the ISGs *Ifit1* and *Cxcl10* were measured by RT-qPCR. Top graph was repeated with indicated n values, and the bottom graph only had single replicates (n=1).

### 3.2.5 UV-inactivating BHV-1 leads to a dose-dependent reduction in viral replication

To determine which amount of UV energy was required to inactivate BHV-1 at concentrations needed for *in vitro* experiments, BHV-1 was diluted to  $3 \times 10^6$  PFU/mL and inactivated at different energies inside a UV crosslinker. This concentration was chosen because  $3 \times 10^6$  PFU/mL approximates an MOI of 10 for our *in vitro* assays. The inactivation range of 0-500mJ/cm<sup>2</sup> was chosen because our lab's HSV-1 preps, an alphaherpesvirus like BHV-1, have historically required energies around 250mJ/cm<sup>2</sup> to be inactivated (data not published). While UV inactivating BHV-1 at  $3 \times 10^6$  PFU/mL demonstrated a dose-dependent response, there is an observable correlation between increasing UV energy and inactivation until a threshold is reached in which we fail to observe additional inactivation (Figure 4). Results from the multiple plaque assays measuring BHV-1 replication following different amounts of UV energy treatment show that 350 mJ/cm<sup>2</sup> was enough UV energy to reduce virus titer a minimum of 10<sup>5</sup>-fold, which aligns with our lab's historic definition of UV-inactivated HSV-1<sup>16</sup>. As further elaborated on in the discussion, however, it is important optimize inactivation conditions for each new preparation of BHV-1. When optimizing the conditions to UV inactivate BHVgIgE, 450mJ/cm<sup>2</sup> was found to be the amount of UV needed.

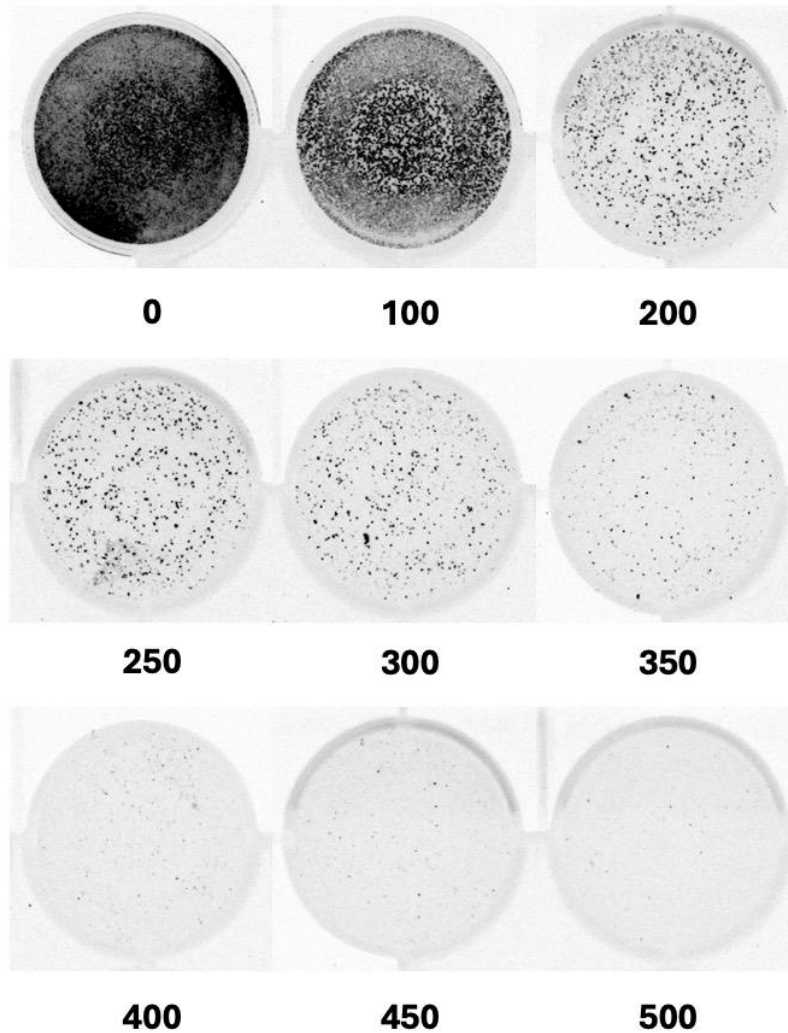


**Figure 4. Effect of different UV intensities on BHV-1 replication.**

Images show CRIB cells infected with live ( $0 \text{ mJ/cm}^2$ ) or UV-inactivated ( $100\text{-}500 \text{ mJ/cm}^2$ ) BHV-1 expressing GFP. Black dots are areas where GFP is detected.  $350 \text{ mJ/cm}^2$  was enough UV energy to reduce this BHV-1 preparation's titer  $10^5$ -fold. All numbers on the images are in  $\text{mJ/cm}^2$ .

### 3.2.6 UV-inactivated BHV-1 induces significantly more ISG expression compared to live BHV-1

Repeated experiments of C10 cells infected with live or UV BHVgIgE showed that 450mJ/cm<sup>2</sup> UV BHVgIgE induced significantly stronger expression of the ISGs *Ifit1* and *Cxcl10* compared to live BHVgIgE. Further, these experiments showed that doubling the UV energy to 900 mJ/cm<sup>2</sup> leads to a similar outcome for *Cxcl10*, but not *Ifit1*. *Cxcl10* expression was significantly higher in 900mJ/cm<sup>2</sup> UV BHVgIgE-treated cells compared to live BHVgIgE-treated cells, whereas *Ifit1* expression was not significantly different between the 900mJ/cm<sup>2</sup> UV BHVgIgE-treated cells and live BHVgIgE-treated cells.

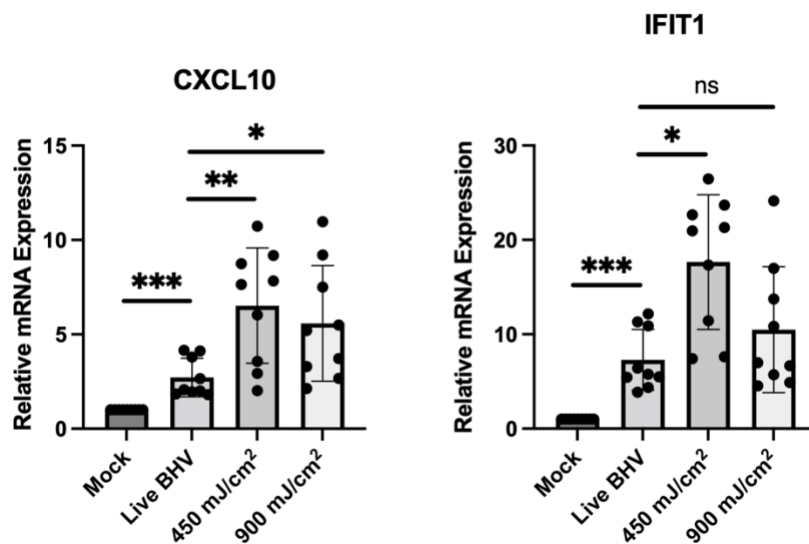


**Figure 5. Induced expression of ISGs in C10 cells after infection with live and UV BHV-1 at 6hpi.**

Mouse melanoma C10 cells were either mock-treated (no virus), treated with MOI 10 live BHVgIgE, or equivalent volume of UV BHVgIgE using two UV<sub>254</sub> intensities (450 mJ/cm<sup>2</sup> or 900 mJ/cm<sup>2</sup>). Relative gene expression of the ISGs *Ifit1* and *Cxcl10* were measured by RT-qPCR. This experiment was repeated 3 times, each time with 3 technical replicates.

\*, p<0.05; \*\*, p<0.01, \*\*\* p<0.001.

### **3.3 700mJ/cm<sup>2</sup> of UV is enough to inactivate BHV-1 at concentrations needed for *in vivo* experiments**

Given how *in vivo* experiments require higher concentrations of BHV-1 ( $4 \times 10^8$  PFU/mL), a new UV optimization for that concentration was essential. A BHV-1 stock aliquot was diluted to  $4 \times 10^8$  PFU/mL and UV-inactivated at 700 mJ/cm<sup>2</sup>. This energy was chosen because UV-inactivating a previous preparation of BHV-1 with this amount of energy at this concentration resulted in no GFP expression in infected CRIB cells. As previously stated, however, not all BHV-1 preparations UV-inactivate at the same energies. The plaque assay of the inactivation for this new preparation that was used for all *in vivo* experiments in the present study (Figure 6a) showed that GFP can still be seen at low levels at the  $10^{-2}$  dilution, though there is an overall estimated 5-log reduction in titer compared to live BHV-1. As shown in the growth curve in Figure 6b, 700mJ/cm<sup>2</sup> of UV is enough to inhibit BHV-1's replication capacity as there is no detectable virus on any of the days of the growth curve. Further, day 2 was the peak of virus titer in both CRIB and C10 cells. Both CRIB and C10 cells were used because CRIB cells are permissive to BHV-1 infection, so they would be the most sensitive to detect live virus, and C10 cells were used to gauge how much replication may happen inside a C10 tumour.

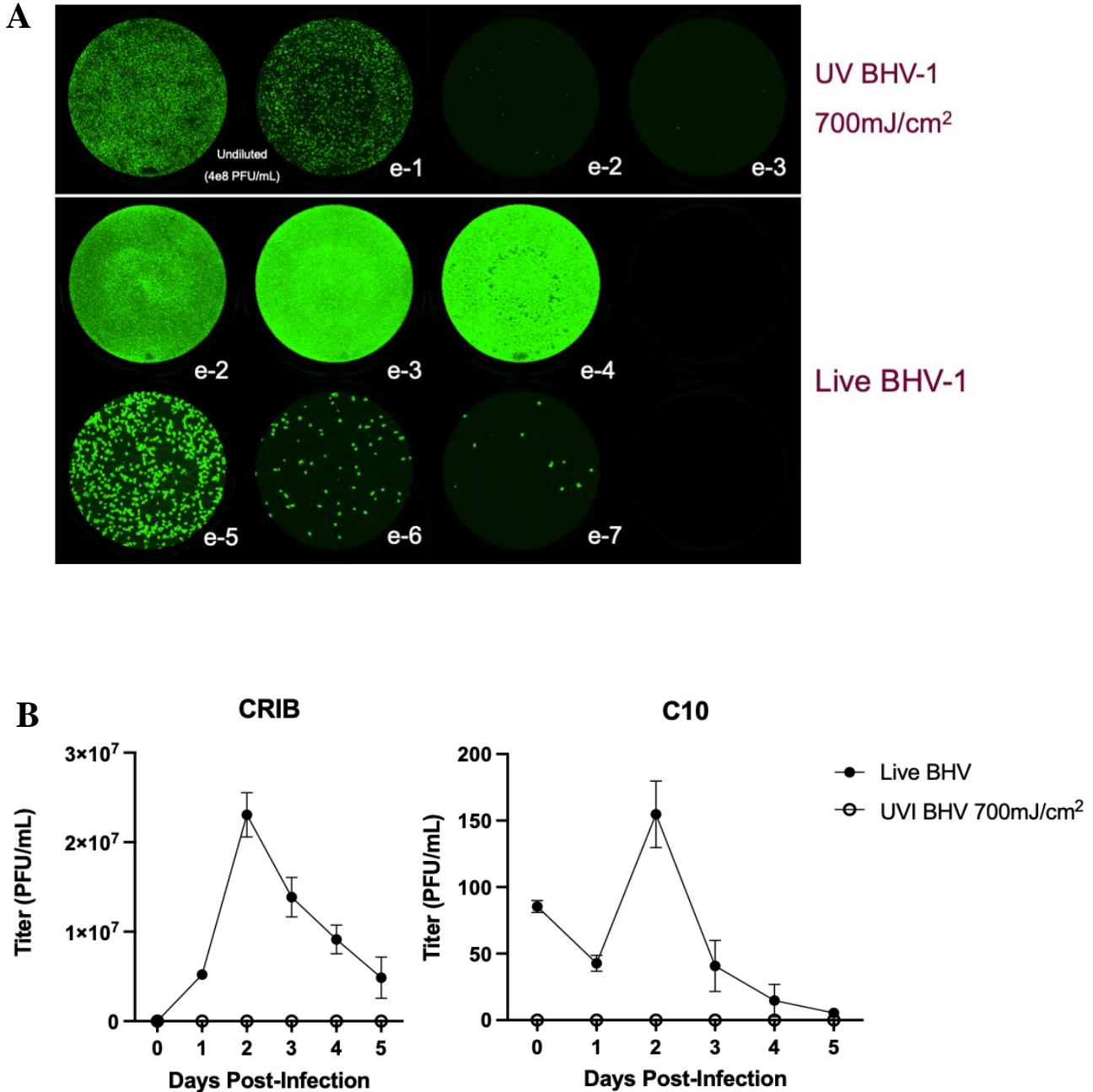


**Figure 6. Plaque assay and growth curve analysis of live and UV-Inactivated BHV-1.**

(A) Plaque assay using CRIB cells showing serial dilutions of 700mJ/cm<sup>2</sup> UV BHV-1 and live BHV-1 originally at 4x10<sup>8</sup> PFU/mL. The results demonstrate a notable ~5-log reduction in titer. (B) Growth curve analysis of CRIB and C10 cells infected with either live or 700mJ/cm<sup>2</sup> UV-treated BHV-1 at a concentration of 4x10<sup>8</sup> PFU/mL with a standard MOI of 0.1. Results show that 700mJ/cm<sup>2</sup> was enough to inhibit BHV-1 replication at the concentration of 4x10<sup>8</sup> PFU/mL. The growth curve was done once with 3 technical replicates, and the plaque assay only once with a single replicate.



### **3.4 UV BHV-1 is as effective as live BHV-1 at extending survival of tumour-bearing mice**

The goal of this experiment was to determine whether live and UV BHV-1 have similar effects on the regression of mouse C10 tumours, and thus definitively test whether BHV-1 needs to replicate to be a viable therapeutic. The schematic for this experiment is outlined in Figure 7a, which is based on our published triple-combination therapeutic regimen.<sup>65</sup> Treatment of C57/B16 mice bearing C10 tumours treated with either live or UV BHV-1 shows no difference in survival. Both groups, however, have significantly longer survival compared to PBS-treated mice ( $p < 0.001$ ; Figure 7b). The average tumour volumes (Figure 7c) and individual tumour growth curves (Figure 7d) of mice treated with either live or UV BHV-1 have similar overall growth patterns. Notably, one mouse in the UV group had a complete regression of its tumour, and no tumour developed following a rechallenge of that mouse with new C10 cells (data not shown).

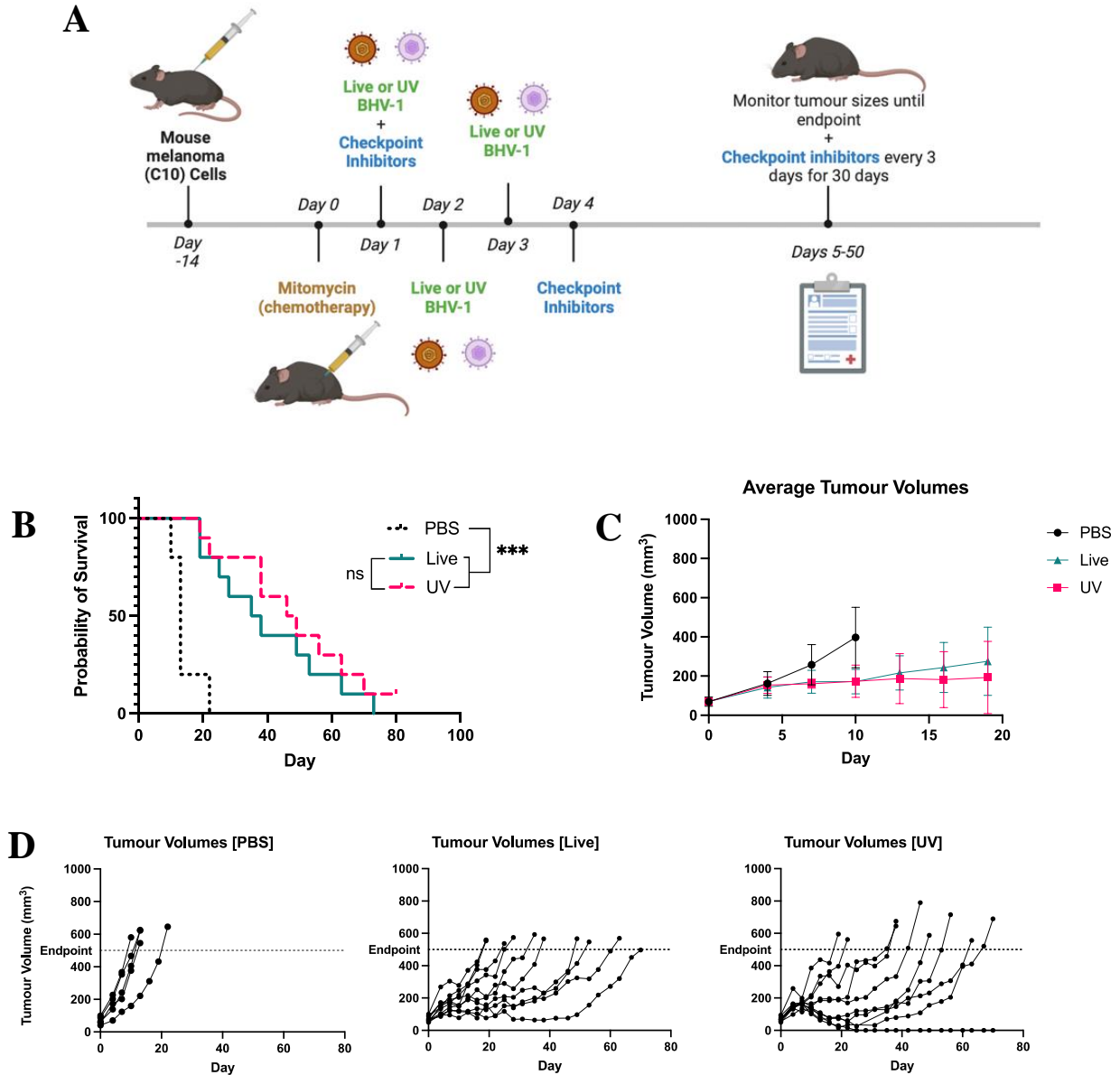


**Figure 7. UV-BHV-1 is as effective as live BHV-1 at extending the survival of mice bearing C10 melanoma tumours.**

(A) Experimental schematic outlining the treatment protocol for C57/Bl6 mice with C10 melanoma tumours, treated either with PBS (n=5), live (n=10) or UV BHV-1 (n=10) as part of a triple-combination therapeutic regimen. (B) Tumour regression survival curve indicating no significant difference in survival between live and UV-BHV-1-treated mice. (C) Average tumour volumes between groups, which show comparable responses in minimizing tumour growth between treatments. (D) Individual tumour growth curves for PBS, live and UV BHV-1-treated mice with one UV-treated mouse exhibiting complete tumour regression. \*\*\*,  $p < 0.001$ .

### **3.5 Live and UV BHV-1-treated tumours have similar immune cell infiltration profiles**

To evaluate which immune cells could be contributing to BHV-1 immunotherapy, mice bearing C10 tumours were treated with either live or UV BHV-1 following the same therapeutic regimen in Figure 7a. On day 10 following the beginning of treatment, tumours were harvested and cells were analyzed using flow cytometry. Results show that live and UV BHV-1 induced significantly more infiltration of cytotoxic T cells (CD3+CD8+), and significantly less infiltration of T regulatory cells (CD3+CD4+FoxP3+) compared to PBS. Tumours treated with live BHV-1 induced significantly more infiltration of neutrophils (CD11b+Ly6G+) compared to PBS-treated tumours, while UV BHV-1-treated tumours had similar infiltration of neutrophils compared to PBS. Neither live nor UV-BHV-1 changed the overall infiltration profile of helper T cells (CD3+CD4+), macrophages (CD11b+F4/80+), or natural killer cells (CD3+NK1.1+).

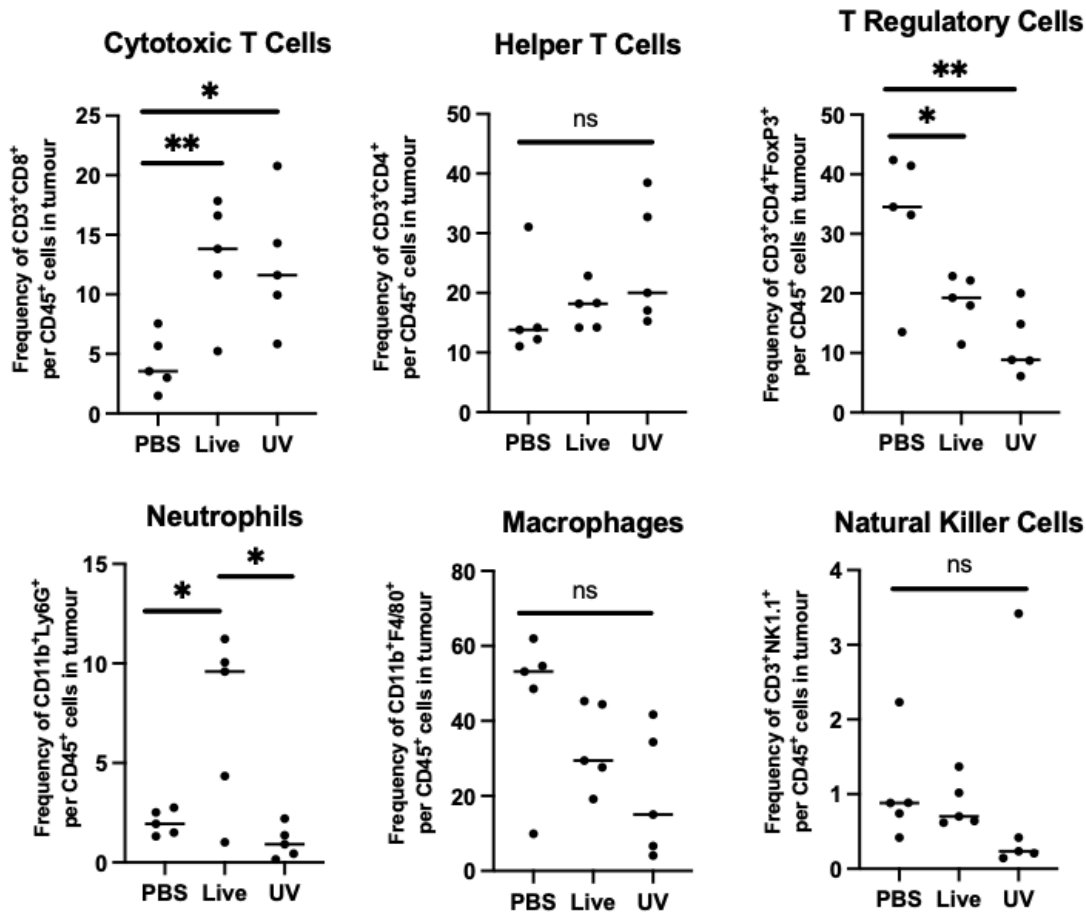


**Figure 8. Tumour infiltration profile of tumours treated with either live or UV BHV-1.**

C57/Bl6 mice with C10 melanoma tumours, treated either with PBS (n=5), live (n=5) or UV (n=5) BHV-1 aligning with the triple-combination therapeutic regimen in Figure 8a. On day 10, tumours were stained and analyzed using flow cytometry. Graphs show the percent (frequency) of immune cell populations per CD45<sup>+</sup> cells in tumours. live BHV-1 and UV BHV-1 induce infiltration of immune cells to a similar degree relative to PBS, with the exception of neutrophils. \*, p < 0.05, \*\* p < 0.01

### **3.6 Live BHV-1 + Mitomycin C and UV BHV-1 + Mitomycin C-treated tumours have similar gene signatures and pathway enrichment profiles**

To better understand the mechanism of action of our therapeutic platform (BHV-1 + Mitomycin C) on a transcriptomic level, mice bearing C10 tumours were treated with UV BHV-1 and data were compared with published findings with live BHV-1.<sup>65</sup> From previous experiments, we know that all three of BHV-1, mito, and checkpoint inhibitors are required together for maximum anti-tumour efficacy.<sup>65</sup> Overall, checkpoint inhibitors are most effective in an “immune hot” microenvironment, while not so effective in “immune cold” microenvironments.<sup>113</sup> The underlying premise of our therapeutic regimen, similar to other viral immunotherapies involving checkpoint inhibitors,<sup>113</sup> is that BHV-1 and mito together are creating an immune microenvironment that allows for our checkpoint inhibitors to be the most effective. Thus, we were interested in understanding what transcriptional changes BHV-1 + mito induces in tumours, and how these changes could be creating an optimal environment for immune checkpoint inhibitors to enact their therapeutic effect. For the present study, we were particularly interested in understanding how these changes are different between live and UV BHV-1. Pathway enrichment analysis of the top 10 signalling pathways showed that the top 8 enriched pathways were identical between tumours treated with mito and live or UV BHV-1, with the exception of their ordinal arrangement (Figure 9a-b). Of particular interest are the pathways associated with chemokine signalling, IL-17A signalling, toll-like receptors, and Type II interferon signalling as these pathways are associated with an immune response. Further, the top 30 differentially expressed genes common between both groups had similar ordinal rankings (Figure 9c). Within each group, the ranking is based on the magnitude of fold change in gene expression, with 1 denoting the gene with the highest fold change in expression for a given group relative to PBS.

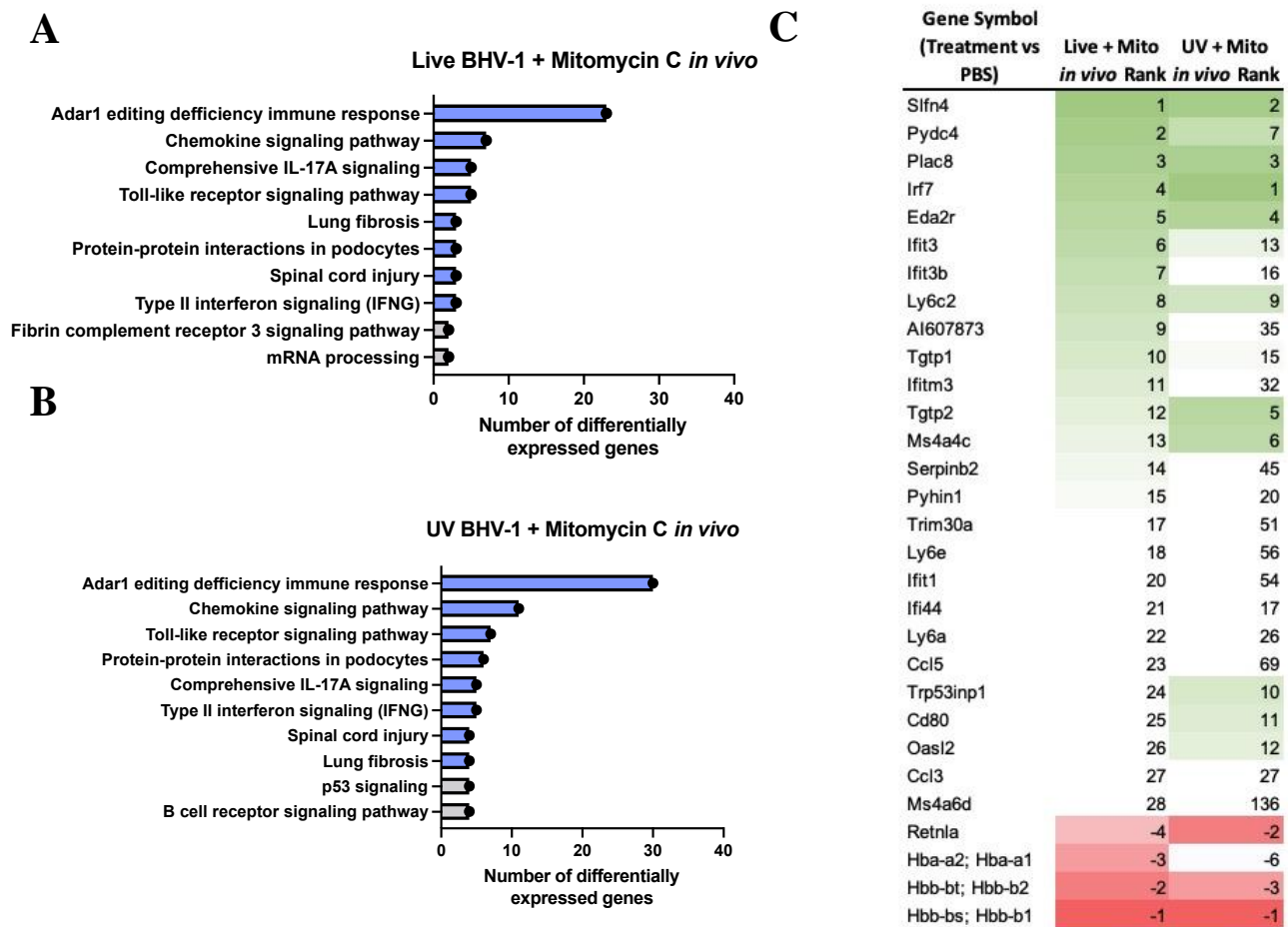


**Figure 9. Pathway enrichment profiles and differentially regulated genes of tumours treated with Mitomycin C and either live or UV BHV-1.**

Left histograms show the pathway enrichment profiles of the top 10 pathways enriched in tumours treated with (A) live BHV-1 + Mitomycin C and (B) UV BHV-1 + Mitomycin C. Histograms shaded in blue represent pathways that are in common between the top 10 enriched pathways in both groups. Grey-shaded pathways happen to still be common between both groups, though have different ordinal ranks that fall outside the top 10. The table on the right (C) lists the ranking of the top 30 differentially regulated genes (>3 fold change) common between tumours treated with Mitomycin C and either live or UV BHV-1. Numbers represent the rank of the relative fold change of each gene. The raw fold change value for each group was the mean value of 5 tumours per group (n=5). Green boxes represent upregulation of gene expression and red boxes represent downregulation.

### **3.7 Live BHV-1 + Mitomycin C and UV BHV-1 + Mitomycin C-treated C10 cells have similar gene signatures and pathway enrichment profiles**

Given the heterogeneity of tumours, it is difficult to attribute pathway enrichments to specific cell types without more precise techniques like single-cell RNA sequencing. To further understand how the Mitomycin C+BHV-1 combination could be impacting C10 cells on their own, though outside of a tumour context, C10 cells were mock infected or infected with live or UV BHV-1 in the presence of Mitomycin C *in vitro*. RNA was harvested at 12 hours post-infection (hpi) across three individual experiments and a microarray was used to analyze the transcriptome. Pathway enrichment analysis showed that of the top 10 enriched pathways, 8 of them were the same between both groups (Figure 10a-b). Of particular interest are pathways involved in B cell receptor signalling and TNF-alpha NF-kB signaling, as these pathways have roles in immunity. Figure 10 indicates the top 15 up-regulated and top 15 down-regulated genes that were common between cells treated with either live BHV-1+mito or UV BHV-1+mito. Of the 790 genes common between both groups, 337 of them were up-regulated and 453 of them were down-regulated.

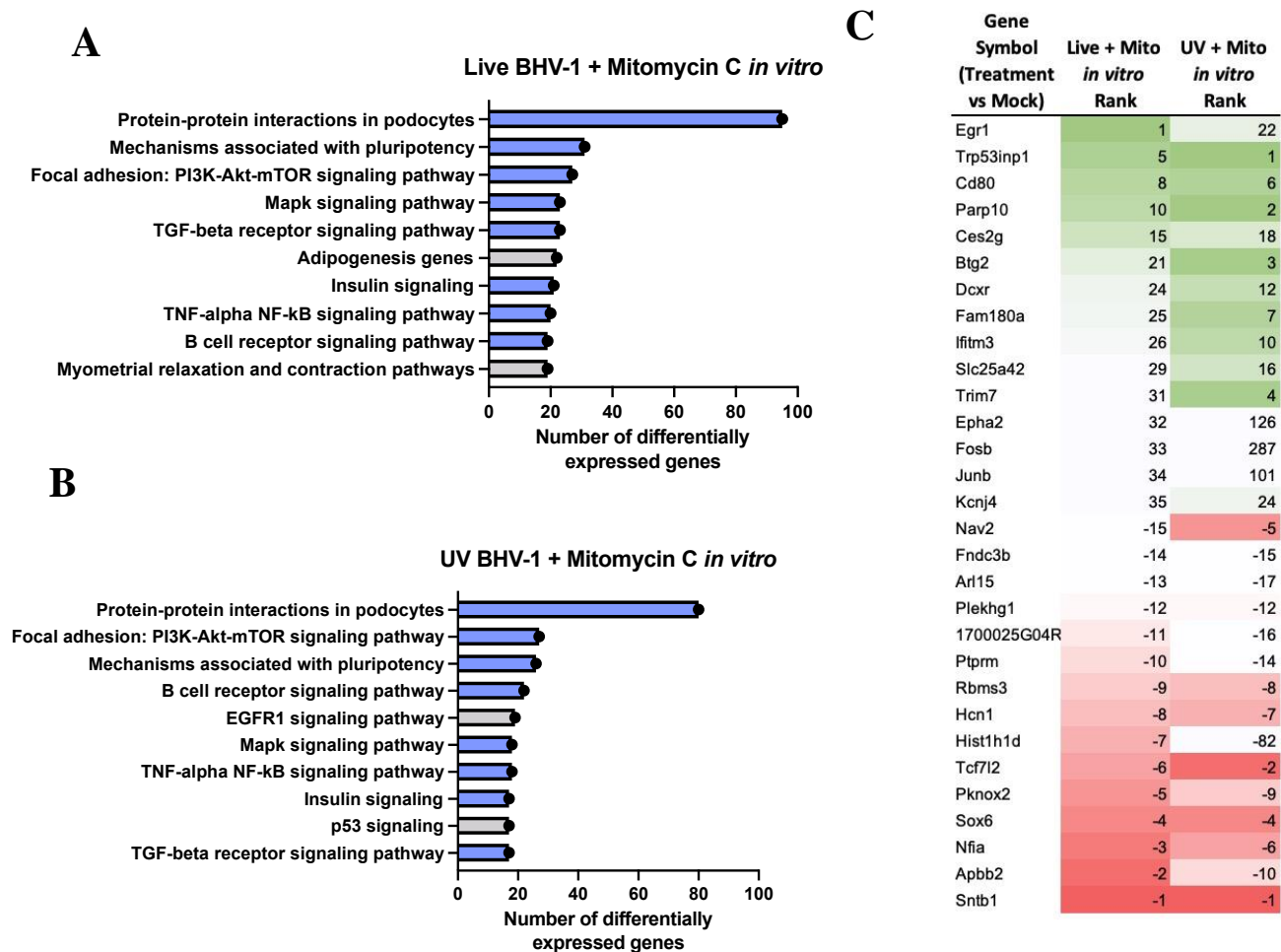


**Figure 10. Pathway enrichment profiles and differentially regulated genes of C10 (B16-hN1) cells treated with Mitomycin C and either live or UV BHV-1 at 12hpi.**

Left histograms show the pathway enrichment profiles of the top 10 pathways enriched in C10 cells treated with (A) live BHV-1 + Mitomycin C and (B) UV BHV-1 + Mitomycin C. Histograms shaded in blue represent pathways that are in common between the top 10 enriched pathways in both groups. Grey-shaded pathways happen to still be common between both groups, though have different ordinal ranks that fall outside the top 10. The table on the right (C) lists the ranking of the top 15 up-regulated genes and top 15 down-regulated genes (>3 fold change) common between both live and UV BHV-1-treated C10 cells. Numbers represent the rank of the relative fold change of each gene. The raw fold change value for each group was the mean value of 3 individual experiments (n=3). Green boxes represent upregulation of gene expression and red boxes represent downregulation.



### **3.8 Only 16 genes comprise BHV-1's "gene signature" in C10 cells across *in vitro* and *in vivo* models**

As further described in the discussion, our lab does not have a reliable screening protocol for new therapeutic regimens where *in vitro* experiments can help us predict outcomes of a given regimen *in vivo*. Thus, to understand if there is a group of genes that is differentially regulated in C10 cells and tumours treated with mito between live and UV BHV-1 across both *in vivo* and *in vitro* contexts, the transcriptome data from all groups were evaluated and compared.

Transcriptome analysis of RNA from tumours harvested on day 5 compared to the same *in vitro* treatment groups with RNA harvested at 12hpi showed 16 genes that were differentially regulated across live BHV-1+mito and UV BHV-1+mito therapeutic treatments, and across *in vivo* vs *in vitro* experiments (Figure 11). About half of the genes were ISGs, many of which are also present in the overlap described in Figure 12, and the other half were related to p53 signalling. These ISGs among many others are expressed downstream of IRF3 signaling, and many other p53-related genes also exist. Therefore, the "signature" for this system across *in vivo* and *in vitro* systems can overall be defined as an IRF3 response and p53 response. As further described in the discussion, this group of genes may help our lab validate new therapy regimens *in vitro* before testing their efficacy *in vivo*. Table 1 briefly describes the role of each gene.

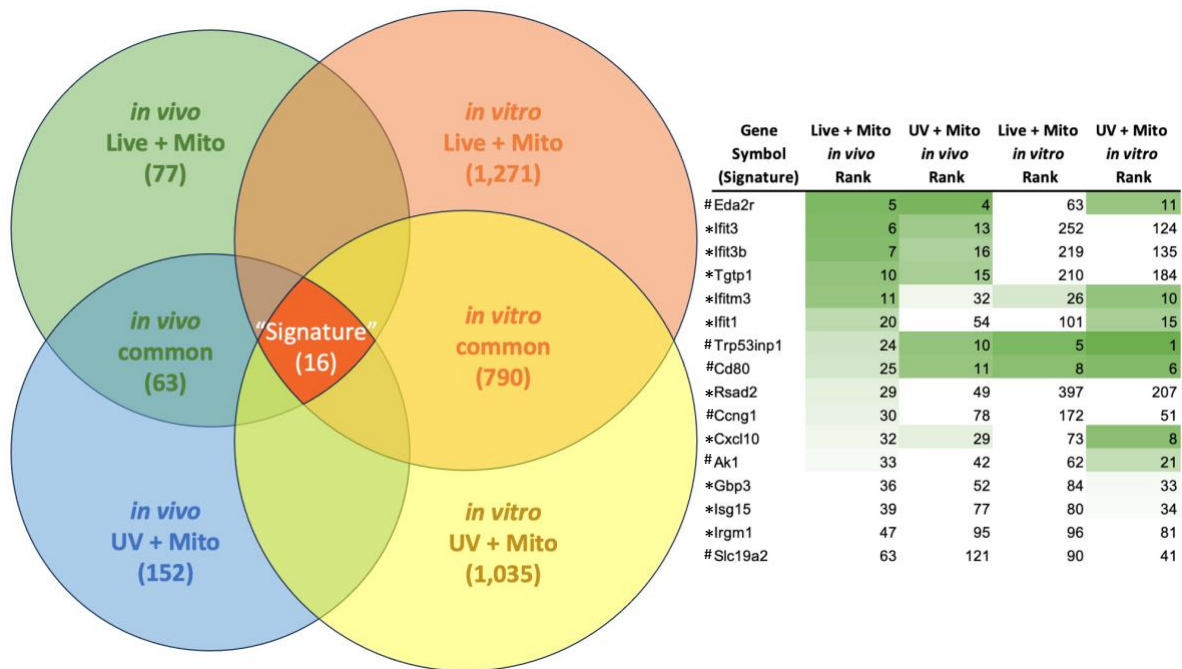


**Figure 11. Schematic diagram of differential gene expression patterns (>3-fold) in C10 (B16-hN1) cells and tumours infected *in vitro* (12hpi) or *in vivo* (5dpi) with live or UV oBHV-1 in the presence of low dose mitomycin C (Mito).**

Values within a given bubble of the Venn diagram represent the number of genes differentially regulated between the indicated group and its respective mock-infected control. “Signature” genes are the genes differentially regulated across live BHV-1 and UV BHV-1 treatments, and across *in vitro* vs *in vivo* experiments all treated with Mitomycin C. The table on the right lists the 16 signature genes and indicates their fold-change ranking within their group. \*IFN-stimulated gene (ISG). #p53-related. All 16 “Signature” genes were upregulated relative to their mock or PBS controls, and there were no down-regulated genes.

<b>Gene</b>	<b>Role</b>
<i>Eda2r</i>	Alias XEDAR: p53-regulated, promoter of apoptosis, inhibitor of cell adhesion transmembrane and member of the TNF receptor superfamily. <sup>114,115</sup>
<i>Ifit3</i>	Forms complex to inhibit viral replication by binding viral RNA. <sup>116</sup> Controversial role in cancer depending on cell type. <sup>117</sup>
<i>Ifit3b</i>	Forms complex to inhibit viral replication by binding viral RNA. <sup>116</sup> Controversial role in cancer depending on cell type. <sup>117</sup>
<i>Tgtp1</i>	Alias T-cell specific GTPase; Involved in response to virus; acts upstream of cellular responses to interferon alpha, beta, and gamma. <sup>118</sup>
<i>Ifitm3</i>	Restricts cellular entry of a variety of viruses; a pan-cancer analysis showed a positive correlation between ifitm3 expression and tumour-infiltration immune cells and immune checkpoints <sup>119</sup>
<i>Ifit1</i>	Forms complex to inhibit viral replication by binding viral RNA. <sup>116</sup> Controversial role in cancer depending on cell type. <sup>117</sup>
<i>Trp53inp1</i>	P53-induced, mediator antioxidant function; absence of TP53INP1 (loss of antioxidant function) favors cancer progression due to ROS. <sup>120</sup>
<i>Cd80</i>	Antigen presentation; CD80 binds both CD28 (stimulating T-cells) and CTLA-4 (inhibiting T-cells), can be induced by p53 in cancer. <sup>121</sup>
<i>Rsad2</i> (viperin)	Inhibits DNA and RNA viral replication. <sup>122</sup> Increased expression correlates with a significant reduction in breast cancer patient survival. <sup>123</sup>
<i>Ccng1</i>	Blocks mitosis when upregulated, cell cycle regulator; transcriptional target of p53. <sup>124</sup>
<i>Cxcl10</i>	Chemokine. Stimulates monocytes, NK, and T cells that can attack cancer. Also associated with tumour development and metastasis. <sup>125</sup>
<i>Ak1</i>	ATP regulation, AK expression is downregulated in several tumours, may be related to oxidative stress; controversial, contains several consensus p53 sites. <sup>126</sup>
<i>Gbp3</i>	Part of the family of guanylate binding proteins; positively correlated with STING expression in human glioblastoma; differential expression from healthy cells differs among cancers. <sup>127</sup>
<i>Isg15</i>	Extracellular immunomodulatory cytokine that regulates cellular function by conjugating proteins. Highly expressed in most tumours. Evidence suggests ISG15 conjugates are protumour but free ISG15 is antitumour. <sup>128</sup>
<i>Irgm1</i>	Immune-related GTPase. Found to increase B16 cell metastasis <i>in vivo</i> and <i>in vitro</i> . <sup>129</sup> Negative regulator of IFN-dependent stimulation of hematopoietic stem cells. <sup>130</sup>
<i>Slc19a2</i>	Solute carrier for B1 (thiamine); target for activation by the p53 tumour suppressor. <sup>131</sup>

**Table 1. Summarized roles of the 16 "Signature" genes.**

### **3.9 Only a small subset of genes is differentially regulated in live and UV BHV-1-infected C10 cells.**

From a biology and molecular virology perspective, we were also interested in understanding the contribution of virus alone in C10 cells. Thus, we analysed the transcriptome of C10 cells infected with live or UV BHV-1 without mito to better understand gene expression dynamics. C10 cells were mock infected or infected with live or UV BHV-1 in the presence of DMSO, which is the vehicle for mito. RNA was harvested 6 and 12 hours post-infection (hpi) and a microarray was used to analyze the transcriptome. Results of the microarray showed several trends among genes that were differentially regulated by UV and live BHV-1 and across both 6hpi and 12hpi. First, live BHV-1 induced the expression of more genes at both 6hpi and 12hpi compared to UV-BHV-1 (Figure 12a). The relative expression of genes between cells treated with either live or UV virus across 6hpi and 12hpi also showed different kinetics: at 6hpi, UV and live BHV-1 induced relatively similar expression levels of genes that were common between live and UV BHV-1, but at 12hpi the expression of genes from cells treated with live BHV-1 was overall higher than those of UV (Figure 12c). Second, the overlap between UV and live BHV-1 contains 9 genes at 6hpi, with 6 of those genes still seen in the overlap at 12hpi (Figure 12b). All but one (*Samd9l*) of the 9 genes were interferon-stimulated genes (ISGs) (Figure 12d). UV BHV-1 only caused the differential expression of 1 unique gene at 6hpi and 2 unique genes at 12hpi (Figure 12a). At 6hpi, the gene was cytidine monophosphate kinase 2 (*Cmpk2*; fold change: 3.8), and at 12hpi the genes were Guanylate binding protein 2 (*Gbp2*; fold change: 3.23) and Gm10663 (fold change: -3.26). Gm10663 is an unannotated gene with no known homologues.

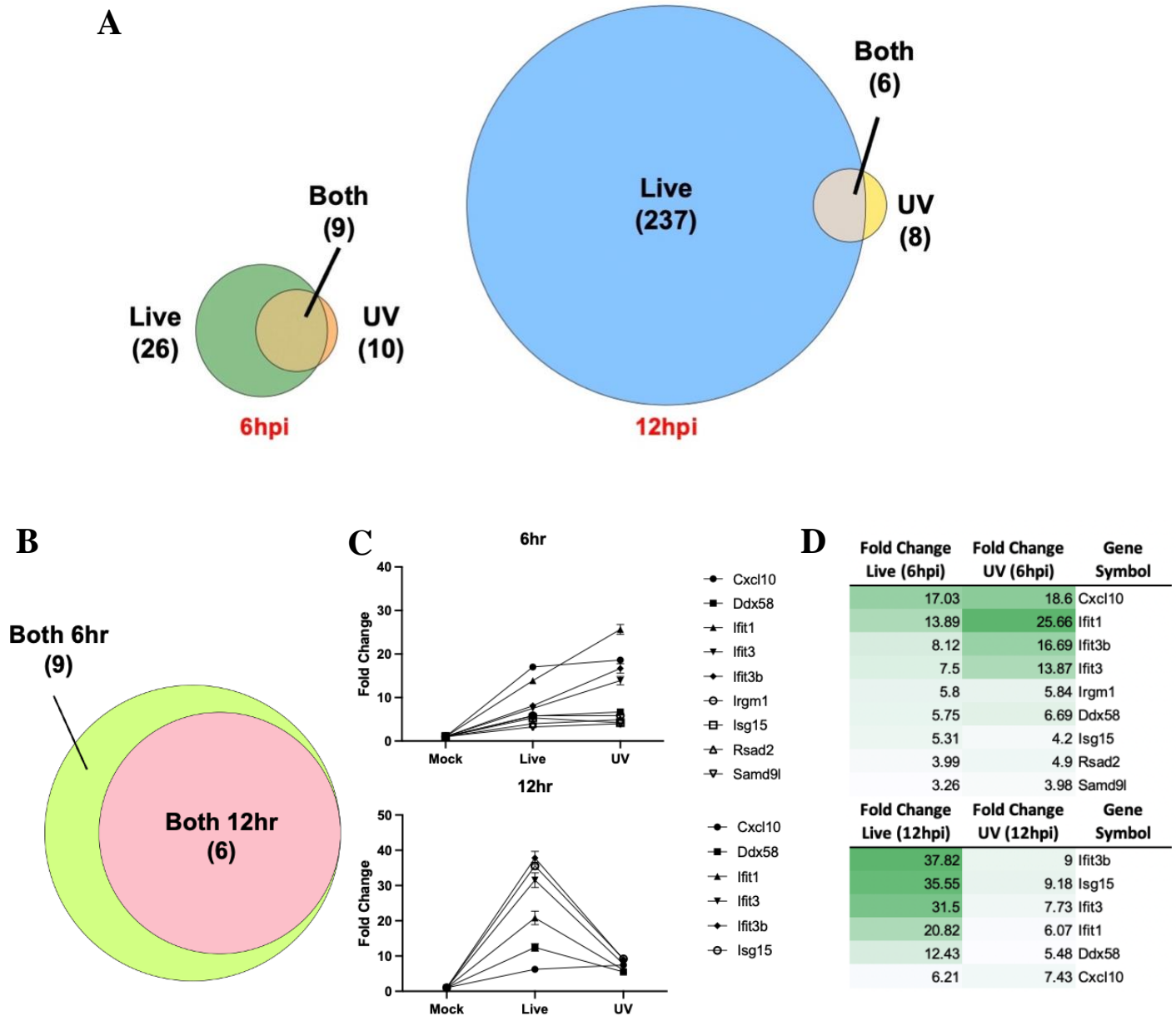


**Figure 12. Differential gene expression patterns in C10 cells infected with UV and live BHV-1 in the presence of DMSO.**

(A) Comparison of gene expression induced by live BHV-1 and UV BHV-1 at 6hpi and 12hpi. live BHV-1 induces the expression of more genes at both time points, reflecting the potential impact of replicating virus triggering additional signalling pathways. (B) Overlap between genes differentially regulated by UV and live BHV-1 at 6hpi, with 9 shared genes, 6 of which remain differentially expressed at 12hpi. (C) Kinetics of relative gene expression between live and UV virus treatments, showing similar expression at 6hpi but higher expression with live BHV-1 at 12hpi. Points on the graphs represent the mean fold change relative to mock and the bars represent the standard deviation. (D) Fold expression values of the 9 shared genes.

## **4. Discussion**

### **4.1 UV BHV-1 as the chosen platform inactivation vector**

The central hypothesis of this project was that non-replicating BHV-1 retains anti-tumour activity. Thus, it was crucial to first develop an inactivated BHV-1 platform to carry out experiments to test this hypothesis. We tried two different methods to inactivate BHV-1: heat inactivation and UV inactivation. Heat inactivation was achieved with different temperatures and durations, though we observed inconsistencies with inactivating using a water bath. As described further in the introduction, we and others have shown that enveloped viruses need to be able to bind and enter into cells to trigger a cellular innate immune response.<sup>15,16,18-22</sup> Given that efficacy of a viral immunotherapy is dependent on immune stimulation, it was necessary to measure whether inactivated BHV-1 retained immune stimulating capacity. While the results from the particle counter showing overlapping histograms of live and HI BHV-1's size distribution suggest that the overall virion integrity was conserved following heat inactivation, heat-inactivated BHV-1 did not induce the expression of ISGs in C10 cells. This lack of ISG induction suggests that the heat treatment may have permanently denatured the envelope proteins required for binding and entering, even though overall virion structure was conserved. After repeated experiments with biological replicates showed observably consistent results of no ISG induction in C10 cells, the decision was made to move on to UV inactivation.

Conversely, UV BHV-1 induces significantly stronger expression of the ISGs *Cxcl10* and *Ifit1* in C10 cells compared to live BHV-1, though my data also suggest that excess UV might eventually abolish this distinction between live and UV BHV-1 (Figure 5). Without viral replication, UV BHV-1 would not be able to express proteins that could dampen the immune

response. The encoded protein ICP0 in particular has been documented in both HSV-1<sup>15</sup> and BHV-1<sup>132</sup> to be critical for disarming key host innate immune defences against virally-infected cells. The significant difference in ISG expression in C10 cells treated with either live BHV-1 and 450mJ/cm<sup>2</sup> UV BHV-1 may be due to BHV-1's inability to produce the viral protein ICP0, which has the ability to reduce cellular levels of IRF3<sup>132</sup>—an upstream factor that stimulates the expression of ISGs like *Cxcl10* and *Ifit1*.<sup>133</sup> By doubling the amount of UV delivered to BHV-1 than was required for inactivation, we also evaluated whether there was an upper limit to BHV-1's capacity to be irradiated yet still induce the expression of ISGs. Treating BHV-1 with higher energies of UV appears to begin diminishing the significant difference in gene expression between UV and live BHV-1 (Figure 5). It is possible that with excess UV radiation, the aromatic residues on glycoprotein D (gD), a protein required for BHV-1 entering, are starting to become altered to a point where gD is losing its conformation to a degree where it cannot support viral entry,<sup>134</sup> though more experiments are needed to confirm these speculations.

One of the caveats of using plaque assays to measure BHV-1's replication is that the GFP expressed by BHV-1 is under a strong constitutive CMV promoter rather than an endogenous BHV-1 promoter. Here, GFP is used as an approximate readout for initiation of replication due to its convenience and our ability to rely on established protocols of measuring replication. While for heat inactivation it was possible to reach a complete reduction in viral titer (i.e. no visible GFP), UV inactivation was not as absolute. Given how UV works by creating crosslinks in DNA, it is possible to imagine a scenario where sufficient crosslinks exist such that the virus cannot complete a full replication cycle, though the GFP coding region remains intact. For this reason, when optimizing conditions for UV-inactivating BHV-1 for *in vivo* experiments, a

growth curve was done to assess viral replication since GFP was still observed in the plaque assay. Further, the majority of the GFP seen in the UV portion of Figure 6a was from single cells as opposed to plaques (data not shown), which further demonstrates the reduced replication capacity of UV BHV-1.

Nearly all of the *in vivo* and *in vitro* experiments used the BHV-1 mutant BHVgfp, though some preliminary experiments (Figure 5) were done with the mutant BHVgIgE. Interestingly, BHVgIgE required higher energies to be inactivated compared to BHVgfp. Even at 999 mJ/cm<sup>2</sup> (the maximum energy that can be delivered by our UV crosslinker at a time), the levels of BHVgIgE replication still did not meet our definition of inactivation when inactivated at the concentration needed for *in vivo* experiments (4x10<sup>8</sup> PFU/mL). The most likely reason for this discrepancy in inactivating energies could be due to the particle:PFU ratio of BHVgIgE. Anecdotally, we have noticed that preparations of BHVgIgE are visibly “cloudier” than preparations of BHVgfp at the same PFU/mL. A preliminary experiment using the Izon qViro Particle Counter showed that a preparation of BHVgIgE has ~7-8x more particles per PFU compared to BHVgfp, though more experiments are needed to confirm exact values. When diluting both BHVgfp and BHVgIgE to 4x10<sup>8</sup> PFU/mL, the concentration used for *in vivo* experiments, the BHVgfp suspension was still observably clearer than the white and cloudy BHVgIgE suspension. The excess particles in the BHVgIgE suspension may prevent the UV from reaching particles at the bottom of the suspension, or they may simply absorb UV light that would otherwise reach live virus particles. A review discussing the use of UV in decontaminating foods summarizes how the turbidity of liquid foods such as skim milk and coconut water can impact how much UV is needed to inactivate microorganisms within the food.



The review further cites how sterilizers should be designed with turbulent flow to maximize the UV exposure of these pathogens.<sup>135</sup> In the present experiments, however, it is impractical to accommodate turbulent flow into the UV inactivation of virus suspensions. The fact that different preparations of virus can have different particle:PFU ratios is not unique to BHV-1. Indeed, this phenomenon has been seen in other viruses from diverse families like Ebola virus,<sup>136</sup> SARS-CoV-2,<sup>137</sup> and adenovirus.<sup>138</sup> Further, since particle:PFU ratios of different preparations of the same BHV-1 mutant can also change, it is important to optimize UV inactivation conditions for individual preparations of BHVgfp and ensure every experiment using a given virus has comparable reductions in viral titer. Indeed, we have found that inactivating different preparations of BHVgfp requires slightly different UV energies, usually in the order of  $\pm 100$  mJ/cm<sup>2</sup> (data not shown). Thus, the UV energy required to inactivate each new preparation of BHV-1 should be optimized.

#### **4.2 Regression of tumours treated with live and UV BHV-1**

One overarching dogma of viral immunotherapies is that the more a virus can replicate, the more effective it should be against tumours, as it would theoretically have a greater capacity to spread and destroy cells. However, as described further in the introduction, replication may not be necessary for viral immunotherapies. Thus, a tumour regression experiment was done to assess the efficacy of UV BHV-1 compared to live BHV-1 in reducing tumour size and inhibiting tumour growth in mice. Since the dilution of BHV-1 to the therapeutic concentration happens before UV-inactivation, this protocol allows for identical quantities of virus particles, some of which are known to be immune-stimulatory,<sup>101</sup> to be used in either the live or UV BHV-1 treatment groups. Overall, the results of this experiment showed that UV BHV-1 is as effective as live BHV-1 at reducing the size of tumours and inhibiting tumour growth. These results align

with previous findings of groups showing the efficacy of inactivated viruses for treating cancers in mouse models,<sup>42,97</sup> and our lab's previous evidence suggesting a lack of correlation between the replication potential of a virus and its therapeutic activity *in vivo*.<sup>96</sup> Further, one mouse treated with UV BHV-1 in the present study had a complete regression of its tumour, which is an outcome previously seen in our lab's experiments with mice treated with live BHV-1 using the present therapeutic regimen (Figure 7d).<sup>65</sup> No tumour developed following a rechallenge of that mouse with new C10 cells, which is another finding consistent with a previous rechallenge study of this model.<sup>65</sup> Even though a single mouse is not enough to draw firm conclusions, this outcome points to UV BHV-1's ability to induce an anti-tumour immune response within mice to make them refractory to rechallenge within our therapeutic regimen.

Even though we now have evidence from this study and others that “cell lysis” is not necessarily a requirement for an anti-tumour effect, the field more broadly still refers to these viruses as “oncolytic viruses.” However, this term must be used with caution and recognition of the caveat that, if there is no “lysis” of cancer cells by the virus, the virus is not truly “oncolytic.” Thus, it would be more appropriate to refer to these therapeutic viruses that do not cause cell lysis as “viral immunotherapies.” This new terminology is more reflective and inclusive of the biology that also involves, and is likely largely dependent on, the stimulation of the host's immune system.

### **4.3 Analysis of Tumour-infiltrating Immune Cells**

The first aim of this experiment was to determine whether the tumour infiltration patterns of different immune cells of UV BHV-1-treated tumours are the same as the live BHV-1-treated tumours. Further, an ongoing question our lab has is what other immune cells could be supporting BHV-1's therapeutic efficacy. Due to the limited number of lasers and filters that can

be used simultaneously on the CytoFLEX LX Flow Cytometer, and the generally low number of tumour cells available to run two panels, the present panel focused on measuring similar parameters as our lab's aforementioned most recent study<sup>65</sup> in addition to markers looking for the presence of neutrophils, macrophages, and NK cells. While the markers chosen for this study were only informative of the presence of these populations, and not their activity or activation, the results from this experiment could be used as a rationale to further explore these immune cells in future experiments.

In the present study, the infiltration of CD4<sup>+</sup> T cells, NK cells, and macrophages was not significantly different between PBS tumours and tumours treated with either virus. This CD4<sup>+</sup> T cell infiltration profile is in contrast with our lab's previous study which did find a significant increase of CD4<sup>+</sup> T cell infiltration in tumours. However, the variance between data points in the present study was observably greater, which could contribute to why significance was not reached. Overall, these data suggest that differential infiltration of NK cells and macrophages may not be contributing to the overall therapy. However, it is possible that the infiltration profile of these immune cells could change between different days, thus more experiments looking at the relative abundance of these cells at different time points would be warranted to completely rule them out. The infiltration of macrophages also has an observable, though not significant, decrease between both viruses and tumours. If the trend was significant, it could suggest that the virus is partially working by decreasing the number of M1 antitumour macrophages. The CD8<sup>+</sup> T cell infiltration, however, was significantly higher in tumours treated with either UV or live BHV-1 compared to PBS. Further, the FoxP3<sup>+</sup>CD4<sup>+</sup> Regulatory T cells were significantly lower in tumours treated with either UV or live BHV-1 compared to PBS. Both of these infiltration

patterns align with our previous findings of live BHV-1.<sup>65</sup> Given that the pathway enrichment analyses suggested live BHV-1 and UV BHV-1 work through similar mechanisms (Figure 9a-b), these results provide further evidence of that being the case.

The tumour infiltration of neutrophils, however, was different between both viruses. Indeed, live BHV-1 induced significantly more neutrophils into tumours compared to PBS and compared to UV BHV-1. UV BHV-1 did not induce more neutrophils compared to PBS. One potential explanation for neutrophil infiltration in tumours treated with live BHV-1 could be the mice's response to a productive viral infection, as neutrophils have been known to attack virally-infected cells.<sup>139</sup> One study, however, showed that intraperitoneal administration of poly(I:C) in mice increased the infiltration of neutrophils into livers as much as their replicating virus alone, which would suggest that viral replication is not necessary for neutrophil infiltration into a tissue.<sup>140</sup> Thus, it is possible that the immunosuppressive tumour microenvironment can be modulated by live BHV-1 in a manner that allows for neutrophil infiltration, while UV BHV-1 cannot. Given how only three of the tumours treated with live BHV-1 appeared to have neutrophil infiltration observably different from PBS, and the other two tumours had a similar infiltration frequency to PBS (Figure 8), it is also possible there is a binary “on or off” effect of neutrophil infiltration that live BHV-1 cannot induce in all tumours. Similarly, while our mice models would ideally be genetic clones, not all our mice experience complete regression of their tumours with the same BHV-1 therapy. Indeed, when we stop administering checkpoint inhibitors to mice that did not have a complete tumour regression, the tumours rapidly grow back. Given how there will always be inherent variability in biological systems, greater numbers of mice would help to clarify these outcomes. One limitation of our model is that we

can either do a tumour regression experiment or analyse immune cell infiltration within a given experiment, but not both, thus preventing use from finding correlations between tumour regression and immune cell infiltration. As described further in the introduction, however, we and others have shown that neutrophils are a key component of, and sometimes required, for different viral immunotherapies.<sup>37,38</sup> To our knowledge, no other study has yet performed a head-to-head comparison of neutrophil infiltration into tumours treated with a live or non-replicating viral immunotherapy. Further studies, such as a neutrophil depletion study involving BHV-1, are necessary to further evaluate the significance of different immune cells in the effectiveness of BHV-1 immunotherapy.

#### **4.4 The transcriptome of cells and tumours treated with live versus UV BHV-1**

The mere fact of UV BHV-1 having no replication capacity is indeed likely to induce a vastly different transcriptomic profile in C10 cells compared to its replicating counterpart. From an *in vivo* perspective, given that live and UV BHV-1 have the same effect on tumour regression, it was imperative to study whether they were working through similar mechanisms. These analyses would help us understand what genes are implicated in BHV-1's therapeutic mechanism, and potentially identify gene candidates that help predict *in vivo* outcomes based on *in vitro* gene profiles. Thus, I asked the question, "What is the global transcriptomic difference between C10 cells and tumours infected with either live or UV BHV-1?"

For this thesis, I performed the same experiment our lab has done previously analyzing the transcriptome of live BHV-1,<sup>65</sup> though using UV BHV-1 and compared my transcriptome data with that from the transcriptome of tumours treated with live BHV-1. Comparing the enriched pathways of tumours treated with live vs UV BHV-1, results suggest that live and UV

BHV-1 work through similar mechanisms against tumours (Figure 9a-b). Indeed, of the top 10 enriched pathways in tumours treated with mito and either live or UV BHV-1, 8 of the pathways were identical between both groups. Overall, the data therefore suggest that the 63 differentially regulated genes that were in the overlap between tumours treated with live or UV BHV-1 could be among the most critical genes for BHV-1's therapeutic efficacy. With the present experiments, we can also compare the C10 tumour transcriptome with those from others in our lab who have used the same microarray approach to study live BHV-1 and other viral immunotherapy vectors *in vivo* in other cancers in mice.<sup>30,65,77</sup> Comparing these enriched pathways in the present C10 tumours to the enriched pathways in MC38 (colon cancer) tumours previously treated with an HSV-1 vector with mito and immune checkpoint inhibitors in our lab,<sup>30</sup> 6 of the top 10 enriched pathways in that study are also among the top 10 in the present tumours treated with BHV-1. The notable matching pathways are, from most to least enriched: Adar1 Editing Deficiency Immune Response, Chemokine Signaling Pathway, Type II Interferon Response, and Toll-Like Receptor Signaling Pathway. As discussed in the introduction, all these pathways are an expected response when viruses infect cells and tumours. The pathway Adar1 Editing Deficiency Immune Response in particular was the top enriched pathway in all 3 cases (live BHV-1, UV BHV-1, and HSV-1,<sup>30</sup> all with mito). In a typical non-virally-infected cell, the Adenosine Deaminase Acting on RNA (ADAR) enzyme catalyzes the conversion of adenosine to inosine on double-stranded RNAs, which helps cells reduce the overactivation of dsRNA-sending pathways and avoid autoimmunity.<sup>141</sup> ADAR1 is interferon-inducible and upregulated by many viruses,<sup>142</sup> while its deficiency is associated with autoimmune disorders.<sup>141</sup> In mice, ADAR1 deficiency is embryonically lethal around day 12.5 due to stress-induced apoptotic death of hematopoietic cells.<sup>143</sup> Further, deleting ADAR1 in murine hematopoietic stem cells leads to

the upregulation of a collection of ISGs,<sup>144</sup> suggesting that the dying of mice embryos could be due to aberrant interferon signalling. In the context of our viral immunotherapies, ADAR1 editing deficiency could be one of the strongest overarching driving factors of tumour killing, allowing for strong expression of ISGs. As described in the introduction, the importance of innate immune signalling for viral immunotherapy is underscored by a group that found STING-KO tumours to be less responsive to their HSV-1-based immunotherapy compared to tumours with WT STING.<sup>99</sup> Overall, these results also illustrate the similarities in the anti-tumour mechanisms of BHV-1 and HSV-1-based viral immunotherapies.

As described in the introduction, Mitomycin C (mito) is a chemotherapy drug used in our *in vivo* therapeutic regimen that has shown synergistic anti-tumour effects with BHV-1.<sup>65</sup> This thesis specifically focused on how BHV-1 and mito as a combination affect the transcriptome of cells and tumours, given that we know neither are effective against tumours on their own.<sup>65</sup> However, it is important to recognize that the transcriptome of cells and tumours treated with BHV-1 alone compared to BHV-1 + mito have a vastly different number of differentially expressed genes. Thus, future analyses of this dataset need to be done to understand the precise contribution of mito on a transcriptome level. For example, we could evaluate how mito changes the total number of genes across different time points, how mito affects gene expression between live and UV BHV-1 before mito is introduced, how these changes differ between *in vitro* and *in vivo*, and others. While the focus of this thesis was specifically on how our therapy differs between live and UV BHV-1, the totality of the data still includes appropriate controls, and thus an opportunity, to answer questions like these in the future.

Our lab has historically failed to observe a correlation between a virus' replication capacity *in vitro* and the strength of its anti-tumour effect *in vivo*.<sup>96</sup> For this reason, we performed a 4-way comparison of tumours and C10 cells treated with either UV or live BHV-1, all with Mitomycin C. The overlap of these 4 groups revealed 16 genes, almost all of which were either ISGs or involved in p53 signalling. The goal with the 16 “Signature” genes is to provide a framework for our lab to examine whether their expression in C10 cells could be a useful indicator of the *in vivo* outcomes of new BHV-1 vectors or therapeutic regimens in the future. The next steps for the present work could include experiments that compare the fold change of these genes *in vitro* across different vectors and evaluate different parameters *in vivo* such as tumour regression or immune cell infiltration to determine if any patterns exist between *in vitro* gene expression and *in vivo* outcomes. For example, we could examine whether tumours in our *in vivo* system express a collection of IRF3-dependent genes and/or a collection of genes related to p53 signaling, then test whether lack of expression of those pathways in tumours leads to diminished efficacy. To test whether a generic IRF3 response is predictive of efficacy, for example, IRF3 itself could be knocked out in the C10 cell lines, and that cell line could be used in a regression experiment. Alternatively, we could interrogate each individual gene from Table 1 by knocking out each one in separate C10 cell lines since it is also possible that a generic IRF3 or p53 response is not sufficiently specific to which genes predict efficacy. These experiments could ultimately allow for faster development of new BHV-1 vectors and associated regimens as performing experiments with animal models for each vector may not be needed to estimate these parameters.

Lastly, aside from the rest of the studies that focused on understanding the therapy (BHV-1 + mito), we also analyzed the gene expression kinetics of live and UV BHV-1 on C10 cells alone,



without mito. Results of this analysis first showed that live BHV-1 induced the expression of more genes at both 6hpi and 12hpi compared to UV BHV-1 (Figure 12a), which is expected as a replicating virus would be expressing proteins that could trigger more signalling pathways. In contrast, a UV virus would likely only trigger pathways that respond to the virus' genome, structural components, and what is induced by the entry process itself. The relative expression of genes between cells treated with either live or UV BHV-1 across 6hpi and 12hpi also showed different kinetics: at 6hpi, UV and live BHV-1 induced relatively similar expression levels of genes, but at 12hpi the expression of genes from cells treated with live BHV-1 were overall higher than those of UV BHV-1 (Figure 12c). A possible explanation is that the cells could clear inactivated viruses faster than replicating viruses, whereas a live virus may continue to produce innate immune-stimulatory molecules that perpetually cause the activation of these genes. Lastly, our lab has previously shown that the expression of a group of ISGs can be induced by inactivated HSV-1<sup>15</sup> or simply membrane perturbation,<sup>21</sup> many of which, including *Cxcl10* and *Ifit1*, also appear in Figure 12. These results therefore further validate our lab's previous findings and show that overlapping pathways are induced across different cell types in response to membrane perturbation and non-replicating viruses.

## **5. Conclusion**

This work explored the potential of non-replicating BHV-1 as an immunotherapy and sheds light on aspects of its mechanism. First, we concluded that UV-inactivated BHV-1 is a viable platform for experiments using non-replicating BHV-1. The transcriptomic differences of cells and tumours infected with either live or UV BHV-1 have shown that only a small subset of genes is expressed across both groups and that the enriched pathways profile of both viruses on their own suggests they work through similar mechanisms within tumours. In cells, the overlap of genes between both viruses aligns with historical data of cells infected with non-replicating enveloped viruses. Most notably, this work has shown that BHV-1 does not need to replicate to exhibit therapeutic efficacy in an *in vivo* model. This result aligns with previous findings of non-replicating enveloped viruses being used as immunotherapies in animal models and is promising for a clinical context where an effective non-replicating viral therapy would have an additional safety element. A non-replicating virus, however, would lack the capacity to express therapeutic transgenes, which for other viral immunotherapies are needed to improve their anti-tumour efficacy. Lastly, the immune cells that infiltrate tumours treated with either live or UV BHV-1 are also similar, with the exception of neutrophils, which brings into question the role of this cell type in BHV-1 immunotherapy. Overall, this work helps shine a light on what the minimum requirements are for BHV-1's therapeutic efficacy and contributes to the growing body of evidence showing that replicating of a viral immunotherapy is not correlated to its efficacy.

## **Appendix: Arabinofuranosyl Cytidine (AraC) as a drug to produce BHV-1 L-particles**

As described in the introduction, herpesvirus light particles (L-particles) are capsid-less and genome-less viral particles that only contain envelope and tegument proteins.<sup>101</sup> Given their inability to express immune-suppressing proteins and still remain immune-stimulatory,<sup>101</sup> it is possible they could have anti-tumour effects *in vivo*. While a proportion of particles in a typical BHV-1 preparation are already L-particles, a study showed that the nucleoside analogue and chemotherapy drug arabinofuranosyl cytidine (AraC)<sup>145</sup> can be used to substantially increase the L-particle:PFU ratio in BHV-1 preparations while maintaining the same number of overall virus particles.<sup>102</sup> The study used PCR to demonstrate that AraC-treated cells infected with BHV-1 had fewer viral genomes compared to cells only infected with BHV-1, while the western blot against the major tegument protein VP8 from the same samples had similar levels of VP8. Further, electron microscopy was used to show that these cells were still producing particles with diameters and morphology relatively consistent with L-particles, which is a detail outlined in the dissertation written by the same author.<sup>146</sup> Further, proteomic data comparing preparations of L-particles and live BHV-1 showed that VP5, the major capsid protein, was present in 4-fold lower quantities in L-particles than complete virions. Thus, a side project I worked on was attempting to optimize the production and purification of BHV-1 L-particles so that they could be used our *in vivo* tumour models.

First, I demonstrated AraC's concentration-dependent effect on BHV-1 replication in permissive CRIB cells (Figure 13). My aim from then was to determine whether I could replicate the findings of the original paper before moving onto purifying the L-particles. I hypothesized that CRIB cells infected with live BHV-1 treated with AraC would result in lower levels of VP5

compared to cells without AraC, while the levels of VP8 between samples would remain consistent. To test this hypothesis, I infected CRIB cells with BHV-1 at MOI 5 and used recovery media containing 100µg/mL AraC. Since BHV-1 exists largely intracellularly, cells were washed with PBS and samples were harvested 24hpi. To normalize the protein amount in my gels, I used a Bradford assay to quantify the amount of protein in each sample and loaded 20µg of protein into each well. I first used the BHV-1 and mock samples to optimize VP5 and VP8 antibodies and found that a dilution of 1:2500 worked for both (Figure 14).

Next, I ran two separate gels with all four samples and blotted them against either VP5 or VP8. While the VP5 blot did appear to have slightly less VP5 content in the AraC + BHV-1 lane compared to the BHV-1 only lane, the VP8 blot showed no VP8 at all in either AraC lanes, which is opposite to what was expected (Figure 15a). Additional background bands that had not appeared during the antibody concentration optimization also appeared on this blot. The VP8 blot was repeated two more times, and each time the AraC + BHV-1 lane lacked a visible VP8 band at the expected size while still showing background bands.

Although BHV-1 is present in low levels in the supernatant, I investigated whether the extracellular BHV-1 particles might show the expected pattern of consistent VP8 between BHV-1 infected cells with and without AraC, but lower VP5 in the AraC + BHV-1 cells. If that were the case, it could suggest that the majority of L-particles exist extracellularly, which is not something explored in the original paper. The results from this blot only showed distinct bands in the supernatant from BHV-1 infected cells without AraC, whereas the BHV-1 + AraC supernatant had barely visible bands, which suggests fewer overall viral particles in the supernatant (Figure 15b). In the supernatant blot there is no lane with only AraC because this supernatant was from a separate identical experiment that did not include this group, but from

which I had reserved the supernatant. Given that AraC's primary mechanism of action is through inhibition of DNA replication, regardless of its potential impact on L-particle generation, it makes sense that less overall virus particles would be produced by cells infected with BHV-1 and treated with AraC.<sup>147</sup>

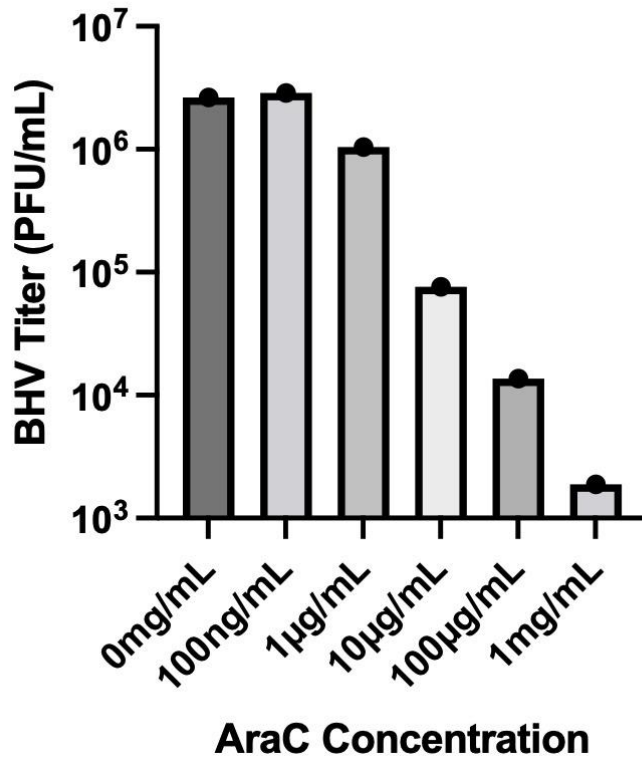


**Figure 13. Effect of arabinofuranosyl cytidine (AraC) on BHV-1 replication.**

Permissive CRIB cells were infected with MOI 5 BHV for 1hr at 37°C. Infection media was then replaced with fresh media containing varying concentrations of AraC. Cells were harvested 24hr post-treatment and a plaque assay using permissive CRIB cells was used to determine titer. The figure shows the results of a single experiment (n=1).

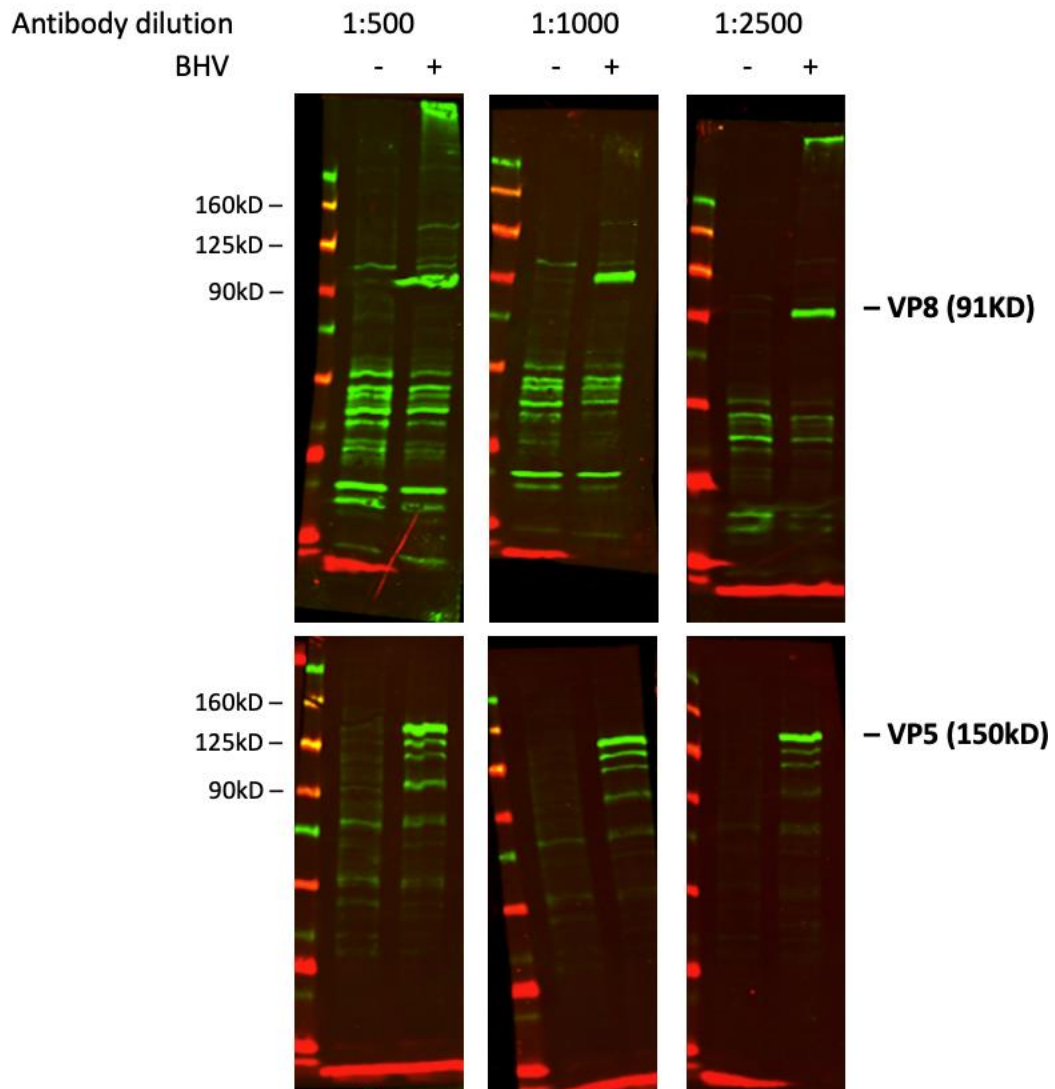


**Figure 14. Concentration optimization of custom VP8 and VP5 antibodies.**

20 $\mu$ g of protein lysates from CRIB cells mock-infected or infected with BHV-1 were blotted with varying concentrations of custom anti-VP8 and anti-VP5 antibodies diluted at either 1:500, 1:1000, or 1:2500. Results indicate that 1:2500 is a reasonable dilution for both antibodies.

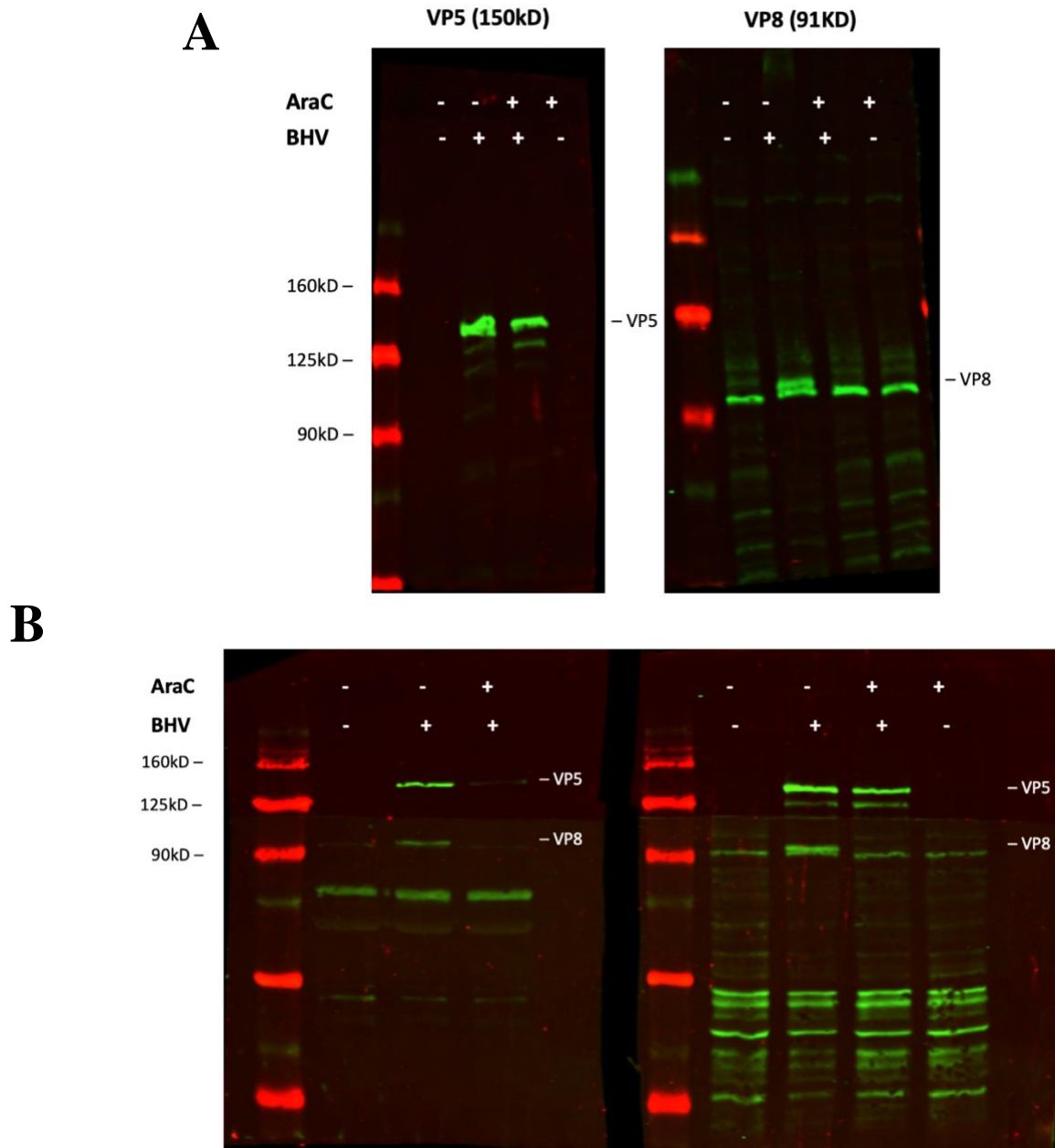


**Figure 15. Western blots targeting the major capsid protein VP5 and major tegument protein VP8.**

(A) Two separate blots were ran using the same protein lysates from CRIB cells mock-infected or infected with BHV-1 and treated or not treated with AraC. Each blot was incubated with primary antibodies against VP5 or VP8. (B) The same lysates from (A) were ran again (right) and supernatants from an identical experiment were ran (left) on different gels. Due to the limited amount of lysate, the nitrocellulose membrane was cut between where VP5 and VP8 were expected to be found, and each half of the membrane was incubated with their respective primary antibodies.

Overall, these results suggest that AraC may be impacting the expression of VP8 rather than VP5, which is opposite to what was previously described. Given that AraC's primary mechanism of action is inhibition of DNA replication,<sup>147</sup> it makes sense that the CRIB cells have an impaired ability to produce virus particles. The reason behind the inhibition of VP8 production, however, is unknown. It is also important to highlight that the original paper discussing the use of AraC to produce L-particles used MDBK cells,<sup>102</sup> which are the parental line to CRIB cells. CRIB cells were originally adapted from MDBK cells to be resistant to Bovine Viral Diarrhea Virus (BVDV) and other pestiviruses.<sup>107</sup> BVDV in particular is a virus found to be contaminated in ATCC's stock of MDBK cells, and also present in low levels of many sources of fetal bovine serum. According to the collaborator from whom we received the CRIB cells, CRIB cells also anecdotally produce lower titers of BHV-1 compared to MDBK cells. For the kind of translational and commercialization research done in our lab, however, it is critical to not have contamination from other viruses in our experiments and preparations, hence why we use CRIB. The adaptive mechanisms behind CRIB cells' resistance to BVDV infection has not been explored by any other group, though the creators of CRIB cells conducted experiments suggesting it might be due to inhibition of BVDV entry.<sup>107</sup> It is possible the mechanisms that make CRIB cells resistant to BVDV infection, and those that anecdotally lead to lower titers than MDBK cells, might be synergizing in some way with AraC, which results in my data being different from the original authors that used AraC to produce L particles from BHV-1 infected MDBK cells. More experiments would have to be done to explore these mechanisms, and ultimately a new protocol needs to be explored to increase the L-particle:PFU ratio in our BHV-1 preparations.



## References

- 1 Zhang, S. & Rabkin, S. D. The discovery and development of oncolytic viruses: are they the future of cancer immunotherapy? *Expert Opin Drug Discov* **16**, 391-410 (2021). <https://doi.org:10.1080/17460441.2021.1850689>
- 2 Bounassar-Filho, J. P., Boeckler-Troncoso, L., Cajigas-Gonzalez, J. & Zavala-Cerna, M. G. SARS-CoV-2 as an Oncolytic Virus Following Reactivation of the Immune System: A Review. *Int J Mol Sci* **24** (2023). <https://doi.org:10.3390/ijms24032326>
- 3 Kelly, E. & Russell, S. J. History of oncolytic viruses: genesis to genetic engineering. *Mol Ther* **15**, 651-659 (2007). <https://doi.org:10.1038/sj.mt.6300108>
- 4 Kim, Y. *et al.* Dendritic Cells in Oncolytic Virus-Based Anti-Cancer Therapy. *Viruses* **7**, 6506-6525 (2015). <https://doi.org:10.3390/v7122953>
- 5 Macedo, N., Miller, D. M., Haq, R. & Kaufman, H. L. Clinical landscape of oncolytic virus research in 2020. *J Immunother Cancer* **8** (2020). <https://doi.org:10.1136/jitc-2020-001486>
- 6 Martuza, R. L., Malick, A., Markert, J. M., Ruffner, K. L. & Coen, D. M. Experimental therapy of human glioma by means of a genetically engineered virus mutant. *Science* **252** (1991).
- 7 Zhao, Y. *et al.* Oncolytic Adenovirus: Prospects for Cancer Immunotherapy. *Front Microbiol* **12**, 707290 (2021). <https://doi.org:10.3389/fmicb.2021.707290>
- 8 Shalhout, S. Z., Miller, D. M., Emerick, K. S. & Kaufman, H. L. Therapy with oncolytic viruses: progress and challenges. *Nat Rev Clin Oncol* **20**, 160-177 (2023). <https://doi.org:10.1038/s41571-022-00719-w>
- 9 Li, Q. *et al.* The gamble between oncolytic virus therapy and IFN. *Front Immunol* **13**, 971674 (2022). <https://doi.org:10.3389/fimmu.2022.971674>
- 10 McNab, F., Mayer-Barber, K., Sher, A., Wack, A. & O'Garra, A. Type I interferons in infectious disease. *Nat Rev Immunol* **15**, 87-103 (2015). <https://doi.org:10.1038/nri3787>
- 11 Sameer, A. S. & Nissar, S. Toll-Like Receptors (TLRs): Structure, Functions, Signaling, and Role of Their Polymorphisms in Colorectal Cancer Susceptibility. *Biomed Res Int* **2021**, 1157023 (2021). <https://doi.org:10.1155/2021/1157023>
- 12 Reikine, S., Nguyen, J. B. & Modis, Y. Pattern Recognition and Signaling Mechanisms of RIG-I and MDA5. *Front Immunol* **5**, 342 (2014). <https://doi.org:10.3389/fimmu.2014.00342>
- 13 Schneider, W. M., Chevillotte, M. D. & Rice, C. M. Interferon-stimulated genes: a complex web of host defenses. *Annu Rev Immunol* **32**, 513-545 (2014). <https://doi.org:10.1146/annurev-immunol-032713-120231>
- 14 Schoggins, J. W. Recent advances in antiviral interferon-stimulated gene biology. *F1000Res* **7**, 309 (2018). <https://doi.org:10.12688/f1000research.12450.1>
- 15 Mossman, K. L. *et al.* Herpes simplex virus triggers and then disarms a host antiviral response. *J Virol* **75**, 750-758 (2001). <https://doi.org:10.1128/JVI.75.2.750-758.2001>
- 16 Collins, S. E., Noyce, R. S. & Mossman, K. L. Innate cellular response to virus particle entry requires IRF3 but not virus replication. *J Virol* **78**, 1706-1717 (2004). <https://doi.org:10.1128/jvi.78.4.1706-1717.2004>
- 17 Weber, M. *et al.* Incoming RNA virus nucleocapsids containing a 5'-triphosphorylated genome activate RIG-I and antiviral signaling. *Cell Host Microbe* **13**, 336-346 (2013). <https://doi.org:10.1016/j.chom.2013.01.012>

- 18 Hare, D. & Mossman, K. L. Novel paradigms of innate immune sensing of viral infections. *Cytokine* **63**, 219-224 (2013). <https://doi.org:10.1016/j.cyto.2013.06.001>
- 19 Hare, D. N., Baid, K., Dvorkin-Gheva, A. & Mossman, K. L. Virus-Intrinsic Differences and Heterogeneous IRF3 Activation Influence IFN-Independent Antiviral Protection. *iScience* **23**, 101864-101864 (2020). <https://doi.org:10.1016/j.isci.2020.101864>
- 20 Hare, D. N. *et al.* Membrane Perturbation-Associated Ca<sup>2+</sup> Signaling and Incoming Genome Sensing Are Required for the Host Response to Low-Level Enveloped Virus Particle Entry. *Journal of Virology* **90**, 3018-3027 (2016). <https://doi.org:10.1128/jvi.02642-15>
- 21 Noyce, R. S. *et al.* Membrane perturbation elicits an IRF3-dependent, interferon-independent antiviral response. *J Virol* **85**, 10926-10931 (2011). <https://doi.org:10.1128/JVI.00862-11>
- 22 Holm, C. K. *et al.* Virus-cell fusion as a trigger of innate immunity dependent on the adaptor STING. *Nat Immunol* **13**, 737-743 (2012). <https://doi.org:10.1038/ni.2350>
- 23 Hare, D. N. *et al.* Membrane Perturbation-Associated Ca<sup>2+</sup> Signaling and Incoming Genome Sensing Are Required for the Host Response to Low-Level Enveloped Virus Particle Entry. *J Virol* **90**, 3018-3027 (2015). <https://doi.org:10.1128/JVI.02642-15>
- 24 Hare, D. N., Baid, K., Dvorkin-Gheva, A. & Mossman, K. L. Virus-Intrinsic Differences and Heterogeneous IRF3 Activation Influence IFN-Independent Antiviral Protection. *iScience* **23**, 101864 (2020). <https://doi.org:10.1016/j.isci.2020.101864>
- 25 McCarthy, E. F. The Toxins of William B. Coley and the Treatment of Bone and Soft-Tissue Sarcomas. *Iowa Orthop J.* **26**, 154-158 (2006).
- 26 Galluzzi, L., Buque, A., Kepp, O., Zitvogel, L. & Kroemer, G. Immunogenic cell death in cancer and infectious disease. *Nat Rev Immunol* **17**, 97-111 (2017). <https://doi.org:10.1038/nri.2016.107>
- 27 Guo, Z. S., Liu, Z. & Bartlett, D. L. Oncolytic Immunotherapy: Dying the Right Way is a Key to Eliciting Potent Antitumor Immunity. *Front Oncol* **4**, 74 (2014). <https://doi.org:10.3389/fonc.2014.00074>
- 28 Filley, A. C. & Dey, M. Immune System, Friend or Foe of Oncolytic Virotherapy? *Front Oncol* **7**, 106 (2017). <https://doi.org:10.3389/fonc.2017.00106>
- 29 Hofman, L., Lawler, S. E. & Lamfers, M. L. M. The Multifaceted Role of Macrophages in Oncolytic Virotherapy. *Viruses* **13** (2021). <https://doi.org:10.3390/v13081570>
- 30 El-Sayes, N. *et al.* A Combination of Chemotherapy and Oncolytic Virotherapy Sensitizes Colorectal Adenocarcinoma to Immune Checkpoint Inhibitors in a cDC1-Dependent Manner. *Int J Mol Sci* **23** (2022). <https://doi.org:10.3390/ijms23031754>
- 31 Oshi, M. *et al.* M1 Macrophage and M1/M2 ratio defined by transcriptomic signatures resemble only part of their conventional clinical characteristics in breast cancer. *Sci Rep* **10**, 16554 (2020). <https://doi.org:10.1038/s41598-020-73624-w>
- 32 Mosser, D. M. & Edwards, J. P. Exploring the full spectrum of macrophage activation. *Nat Rev Immunol* **8**, 958-969 (2008). <https://doi.org:10.1038/nri2448>
- 33 Kleijn, A. *et al.* The in vivo therapeutic efficacy of the oncolytic adenovirus Delta24-RGD is mediated by tumor-specific immunity. *PLoS One* **9**, e97495 (2014). <https://doi.org:10.1371/journal.pone.0097495>
- 34 Kwan, A. *et al.* Macrophages Mediate the Antitumor Effects of the Oncolytic Virus HSV1716 in Mammary Tumors. *Mol Cancer Ther* **20**, 589-601 (2021). <https://doi.org:10.1158/1535-7163.MCT-20-0748>

- 35 Burn, G. L., Foti, A., Marsman, G., Patel, D. F. & Zychlinsky, A. The Neutrophil. *Immunity* **54**, 1377-1391 (2021). <https://doi.org:10.1016/j.immuni.2021.06.006>
- 36 Fridlender, Z. G. *et al.* Polarization of tumor-associated neutrophil phenotype by TGF-beta: "N1" versus "N2" TAN. *Cancer Cell* **16**, 183-194 (2009). <https://doi.org:10.1016/j.ccr.2009.06.017>
- 37 Minott, J. A. *et al.* The Role of Neutrophils in Oncolytic Orf Virus-Mediated Cancer Immunotherapy. *Cells* **11** (2022). <https://doi.org:10.3390/cells11182858>
- 38 Workenhe, S. T., Pol, J. G., Lichty, B. D., Cummings, D. T. & Mossman, K. L. Combining oncolytic HSV-1 with immunogenic cell death-inducing drug mitoxantrone breaks cancer immune tolerance and improves therapeutic efficacy. *Cancer Immunol Res* **1**, 309-319 (2013). <https://doi.org:10.1158/2326-6066.CIR-13-0059-T>
- 39 Wculek, S. K. *et al.* Dendritic cells in cancer immunology and immunotherapy. *Nat Rev Immunol* **20**, 7-24 (2020). <https://doi.org:10.1038/s41577-019-0210-z>
- 40 Durai, V. & Murphy, K. M. Functions of Murine Dendritic Cells. *Immunity* **45**, 719-736 (2016). <https://doi.org:10.1016/j.immuni.2016.10.010>
- 41 Wang, W. *et al.* Elucidating mechanisms of antitumor immunity mediated by live oncolytic vaccinia and heat-inactivated vaccinia. *J Immunother Cancer* **9** (2021). <https://doi.org:10.1136/jitc-2021-002569>
- 42 Dai, P. *et al.* Intratumoral delivery of inactivated modified vaccinia virus Ankara (iMVA) induces systemic antitumor immunity via STING and Batf3-dependent dendritic cells. *Sci Immunol* **2** (2017). <https://doi.org:10.1126/sciimmunol.aal1713>
- 43 Toda, M., Martuza, R. L. & Rabkin, S. D. Tumor growth inhibition by intratumoral inoculation of defective herpes simplex virus vectors expressing granulocyte-macrophage colony-stimulating factor. *Mol Ther* **2**, 324-329 (2000). <https://doi.org:10.1006/mthe.2000.0130>
- 44 Ogbomo, H. *et al.* Myxoma virus infection promotes NK lysis of malignant gliomas in vitro and in vivo. *PLoS One* **8**, e66825 (2013). <https://doi.org:10.1371/journal.pone.0066825>
- 45 Zamarin, D. *et al.* Localized oncolytic virotherapy overcomes systemic tumor resistance to immune checkpoint blockade immunotherapy. *Sci Transl Med* **6**, 226ra232 (2014). <https://doi.org:10.1126/scitranslmed.3008095>
- 46 Wang, Y. *et al.* NK cell tumor therapy modulated by UV-inactivated oncolytic herpes simplex virus type 2 and checkpoint inhibitors. *Transl Res* **240**, 64-86 (2022). <https://doi.org:10.1016/j.trsl.2021.10.006>
- 47 Bhat, R., Dempe, S., Dinsart, C. & Rommelaere, J. Enhancement of NK cell antitumor responses using an oncolytic parvovirus. *Int J Cancer* **128**, 908-919 (2011). <https://doi.org:10.1002/ijc.25415>
- 48 Cibrian, D. & Sanchez-Madrid, F. CD69: from activation marker to metabolic gatekeeper. *Eur J Immunol* **47**, 946-953 (2017). <https://doi.org:10.1002/eji.201646837>
- 49 Verschoor, C. P. *et al.* NK- and T-cell granzyme B and K expression correlates with age, CMV infection and influenza vaccine-induced antibody titres in older adults. *Front Aging* **3**, 1098200 (2022). <https://doi.org:10.3389/fragi.2022.1098200>
- 50 Warricker, F., Khakoo, S. I. & Blunt, M. D. The role of NK cells in oncolytic viral therapy: a focus on hepatocellular carcinoma. *J Transl Genet Genom* **5**, 304-322 (2021). <https://doi.org:10.20517/jtgg.2021.27>

- 51 Akkaya, M., Kwak, K. & Pierce, S. K. B cell memory: building two walls of protection against pathogens. *Nat Rev Immunol* **20**, 229-238 (2020). <https://doi.org:10.1038/s41577-019-0244-2>
- 52 Vito, A. *et al.* Immune checkpoint blockade in triple negative breast cancer influenced by B cells through myeloid-derived suppressor cells. *Commun Biol* **4**, 859 (2021). <https://doi.org:10.1038/s42003-021-02375-9>
- 53 Luo, Y. *et al.* Tumor-targeting oncolytic virus elicits potent immunotherapeutic vaccine responses to tumor antigens. *Oncoimmunology* **9**, 1726168 (2020). <https://doi.org:10.1080/2162402X.2020.1726168>
- 54 Raskov, H., Orhan, A., Christensen, J. P. & Gogenur, I. Cytotoxic CD8(+) T cells in cancer and cancer immunotherapy. *Br J Cancer* **124**, 359-367 (2021). <https://doi.org:10.1038/s41416-020-01048-4>
- 55 Wang, Q., Qin, Y. & Li, B. CD8(+) T cell exhaustion and cancer immunotherapy. *Cancer Lett* **559**, 216043 (2023). <https://doi.org:10.1016/j.canlet.2022.216043>
- 56 Broz, M. L. *et al.* Dissecting the tumor myeloid compartment reveals rare activating antigen-presenting cells critical for T cell immunity. *Cancer Cell* **26**, 638-652 (2014). <https://doi.org:10.1016/j.ccell.2014.09.007>
- 57 Ruffell, B. *et al.* Macrophage IL-10 blocks CD8+ T cell-dependent responses to chemotherapy by suppressing IL-12 expression in intratumoral dendritic cells. *Cancer Cell* **26**, 623-637 (2014). <https://doi.org:10.1016/j.ccell.2014.09.006>
- 58 Philip, M. & Schietinger, A. CD8(+) T cell differentiation and dysfunction in cancer. *Nat Rev Immunol* **22**, 209-223 (2022). <https://doi.org:10.1038/s41577-021-00574-3>
- 59 Kurachi, M. CD8(+) T cell exhaustion. *Semin Immunopathol* **41**, 327-337 (2019). <https://doi.org:10.1007/s00281-019-00744-5>
- 60 Lovatt, C. & Parker, A. L. Oncolytic Viruses and Immune Checkpoint Inhibitors: The "Hot" New Power Couple. *Cancers (Basel)* **15** (2023). <https://doi.org:10.3390/cancers15164178>
- 61 Tay, R. E., Richardson, E. K. & Toh, H. C. Revisiting the role of CD4(+) T cells in cancer immunotherapy-new insights into old paradigms. *Cancer Gene Ther* **28**, 5-17 (2021). <https://doi.org:10.1038/s41417-020-0183-x>
- 62 Hor, J. L. *et al.* Spatiotemporally Distinct Interactions with Dendritic Cell Subsets Facilitates CD4+ and CD8+ T Cell Activation to Localized Viral Infection. *Immunity* **43**, 554-565 (2015). <https://doi.org:10.1016/j.immuni.2015.07.020>
- 63 Quezada, S. A. *et al.* Tumor-reactive CD4(+) T cells develop cytotoxic activity and eradicate large established melanoma after transfer into lymphopenic hosts. *J Exp Med* **207**, 637-650 (2010). <https://doi.org:10.1084/jem.20091918>
- 64 Lindqvist, C. A. *et al.* T regulatory cells control T-cell proliferation partly by the release of soluble CD25 in patients with B-cell malignancies. *Immunology* **131**, 371-376 (2010). <https://doi.org:10.1111/j.1365-2567.2010.03308.x>
- 65 Davola, M. E. *et al.* Oncolytic BHV-1 Is Sufficient to Induce Immunogenic Cell Death and Synergizes with Low-Dose Chemotherapy to Dampen Immunosuppressive T Regulatory Cells. *Cancers (Basel)* **15** (2023). <https://doi.org:10.3390/cancers15041295>
- 66 Todo, T. *et al.* Intratumoral oncolytic herpes virus G47 $\Delta$  for residual or recurrent glioblastoma: a phase 2 trial. *Nat Med* **28**, 1630-1639 (2022). <https://doi.org:10.1038/s41591-022-01897-x>

- 67 Nair, A., Chauhan, P., Saha, B. & Kubatzky, K. F. Conceptual Evolution of Cell  
 Signaling. *Int J Mol Sci* **20** (2019). <https://doi.org:10.3390/ijms20133292>
- 68 Alemohammad, H. *et al.* The importance of immune checkpoints in immune monitoring:  
 A future paradigm shift in the treatment of cancer. *Biomed Pharmacother* **146**, 112516  
 (2022). <https://doi.org:10.1016/j.biopha.2021.112516>
- 69 Immune Checkpoint Inhibitors. (2022). <https://doi.org:https://www.cancer.gov/about-cancer/treatment/types/immunotherapy/checkpoint-inhibitors>
- 70 Zou, H., Mou, X. Z. & Zhu, B. Combining of Oncolytic Virotherapy and Other  
 Immunotherapeutic Approaches in Cancer: A Powerful Functionalization Tactic. *Glob  
 Chall* **7**, 2200094 (2023). <https://doi.org:10.1002/gch2.202200094>
- 71 Jenkins, R. W., Barbie, D. A. & Flaherty, K. T. Mechanisms of resistance to immune  
 checkpoint inhibitors. *Br J Cancer* **118**, 9-16 (2018).  
<https://doi.org:10.1038/bjc.2017.434>
- 72 Beyer, M. *et al.* Reduced frequencies and suppressive function of CD4+CD25hi  
 regulatory T cells in patients with chronic lymphocytic leukemia after therapy with  
 fludarabine. *Blood* **106**, 2018-2025 (2005). <https://doi.org:10.1182/blood-2005-02-0642>
- 73 Zhang, L. *et al.* Differential impairment of regulatory T cells rather than effector T cells  
 by paclitaxel-based chemotherapy. *Clin Immunol* **129**, 219-229 (2008).  
<https://doi.org:10.1016/j.clim.2008.07.013>
- 74 Nguyen, A., Ho, L. & Wan, Y. Chemotherapy and Oncolytic Virotherapy: Advanced  
 Tactics in the War against Cancer. *Front Oncol* **4**, 145 (2014).  
<https://doi.org:10.3389/fonc.2014.00145>
- 75 Esaki, S., Goshima, F., Kimura, H., Murakami, S. & Nishiyama, Y. Enhanced  
 antitumoral activity of oncolytic herpes simplex virus with gemcitabine using colorectal  
 tumor models. *Int J Cancer* **132**, 1592-1601 (2013). <https://doi.org:10.1002/ijc.27823>
- 76 Takehara, Y. *et al.* Anti-tumor effects of inactivated Sendai virus particles with an IL-2  
 gene on angiosarcoma. *Clin Immunol* **149**, 1-10 (2013).  
<https://doi.org:10.1016/j.clim.2013.05.019>
- 77 Vito, A., El-Sayes, N., Salem, O., Wan, Y. & Mossman, K. L. Response to FEC  
 Chemotherapy and Oncolytic HSV-1 Is Associated with Macrophage Polarization and  
 Increased Expression of S100A8/A9 in Triple Negative Breast Cancer. *Cancers (Basel)*  
**13** (2021). <https://doi.org:10.3390/cancers13215590>
- 78 Workenhe, S. T. *et al.* De novo necroptosis creates an inflammatory environment  
 mediating tumor susceptibility to immune checkpoint inhibitors. *Commun Biol* **3**, 645  
 (2020). <https://doi.org:10.1038/s42003-020-01362-w>
- 79 Liu, X. *et al.* Efficacy and safety of oncolytic virus combined with chemotherapy or  
 immune checkpoint inhibitors in solid tumor patients: A meta-analysis. *Front Pharmacol*  
**13**, 1023533 (2022). <https://doi.org:10.3389/fphar.2022.1023533>
- 80 Jones, C. Bovine Herpesvirus 1 Counteracts Immune Responses and Immune-  
 Surveillance to Enhance Pathogenesis and Virus Transmission. *Front Immunol* **10**, 1008  
 (2019). <https://doi.org:10.3389/fimmu.2019.01008>
- 81 Rodrigues, R., Cuddington, B. & Mossman, K. Bovine herpesvirus type 1 as a novel  
 oncolytic virus. *Cancer Gene Ther* **17**, 344-355 (2010).  
<https://doi.org:10.1038/cgt.2009.77>
- 82 Cuddington, B. P., Dyer, A. L., Workenhe, S. T. & Mossman, K. L. Oncolytic bovine  
 herpesvirus type 1 infects and kills breast tumor cells and breast cancer-initiating cells

- irrespective of tumor subtype. *Cancer Gene Ther* **20**, 282-289 (2013).  
<https://doi.org:10.1038/cgt.2013.18>
- 83 Cuddington, B. P. & Mossman, K. L. Permissiveness of human cancer cells to oncolytic bovine herpesvirus 1 is mediated in part by KRAS activity. *J Virol* **88**, 6885-6895 (2014).  
<https://doi.org:10.1128/JVI.00849-14>
- 84 Qiu, W., Ding, X., Li, S., He, Y. & Zhu, L. Oncolytic Bovine Herpesvirus 1 Inhibits Human Lung Adenocarcinoma A549 Cell Proliferation and Tumor Growth by Inducing DNA Damage. *Int J Mol Sci* **22** (2021). <https://doi.org:10.3390/ijms22168582>
- 85 Mann, B. S., Johnson, J. R., Cohen, M. H., Justice, R. & Pazdur, R. FDA approval summary: vorinostat for treatment of advanced primary cutaneous T-cell lymphoma. *Oncologist* **12**, 1247-1252 (2007). <https://doi.org:10.1634/theoncologist.12-10-1247>
- 86 Kim, S. I. *et al.* Recombinant Orthopoxvirus Primes Colon Cancer for Checkpoint Inhibitor and Cross-Primes T Cells for Antitumor and Antiviral Immunity. *Mol Cancer Ther* **20**, 173-182 (2021). <https://doi.org:10.1158/1535-7163.MCT-20-0405>
- 87 Meisen, W. H. *et al.* The Impact of Macrophage- and Microglia-Secreted TNFalpha on Oncolytic HSV-1 Therapy in the Glioblastoma Tumor Microenvironment. *Clin Cancer Res* **21**, 3274-3285 (2015). <https://doi.org:10.1158/1078-0432.CCR-14-3118>
- 88 Saha, D., Martuza, R. L. & Rabkin, S. D. Macrophage Polarization Contributes to Glioblastoma Eradication by Combination Immunovirotherapy and Immune Checkpoint Blockade. *Cancer Cell* **32**, 253-267 e255 (2017).  
<https://doi.org:10.1016/j.ccell.2017.07.006>
- 89 Yoo, J. Y. *et al.* Bortezomib-induced unfolded protein response increases oncolytic HSV-1 replication resulting in synergistic antitumor effects. *Clin Cancer Res* **20**, 3787-3798 (2014). <https://doi.org:10.1158/1078-0432.CCR-14-0553>
- 90 Lee, S. *et al.* Inhibition of MEK-ERK pathway enhances oncolytic vaccinia virus replication in doxorubicin-resistant ovarian cancer. *Mol Ther Oncolytics* **25**, 211-224 (2022). <https://doi.org:10.1016/j.omto.2022.04.006>
- 91 Doronin, K. *et al.* Tumor-specific, replication-competent adenovirus vectors overexpressing the adenovirus death protein. *J Virol* **74**, 6147-6155 (2000).  
<https://doi.org:10.1128/jvi.74.13.6147-6155.2000>
- 92 Guo, Z. S. *et al.* The combination of immunosuppression and carrier cells significantly enhances the efficacy of oncolytic poxvirus in the pre-immunized host. *Gene Ther* **17**, 1465-1475 (2010). <https://doi.org:10.1038/gt.2010.104>
- 93 Ikeda, K. *et al.* Oncolytic virus therapy of multiple tumors in the brain requires suppression of innate and elicited antiviral responses. *Nat Med* **5**, 881-887 (1999).  
<https://doi.org:10.1038/11320>
- 94 Davola, M. E. & Mossman, K. L. Oncolytic viruses: how "lytic" must they be for therapeutic efficacy? *Oncoimmunology* **8**, e1581528 (2019).  
<https://doi.org:10.1080/2162402X.2019.1596006>
- 95 Bell, J. & McFadden, G. Viruses for tumor therapy. *Cell Host Microbe* **15**, 260-265 (2014). <https://doi.org:10.1016/j.chom.2014.01.002>
- 96 Workenhe, S. T. *et al.* Immunogenic HSV-mediated oncolysis shapes the antitumor immune response and contributes to therapeutic efficacy. *Mol Ther* **22**, 123-131 (2014).  
<https://doi.org:10.1038/mt.2013.238>
- 97 Samudio, I. *et al.* UV-inactivated HSV-1 potently activates NK cell killing of leukemic cells. *Blood* **127**, 2575-2586 (2016). <https://doi.org:10.1182/blood-2015-04-639088>

- 98 Samudio, I. *et al.* UV Light-inactivated HSV-1 Stimulates Natural Killer Cell-induced Killing of Prostate Cancer Cells. *J Immunother* **42**, 162-174 (2019). <https://doi.org:10.1097/CJI.0000000000000261>
- 99 Froeulich, G. *et al.* Integrity of the Antiviral STING-mediated DNA Sensing in Tumor Cells Is Required to Sustain the Immunotherapeutic Efficacy of Herpes Simplex Oncolytic Virus. *Cancers (Basel)* **12** (2020). <https://doi.org:10.3390/cancers12113407>
- 100 Gamble, A. *et al.* Heat-treated virus inactivation rate depends strongly on treatment procedure: illustration with SARS-CoV-2. *bioRxiv* (2021). <https://doi.org:10.1101/2020.08.10.242206>
- 101 Heilingloh, C. S. & Krawczyk, A. Role of L-Particles during Herpes Simplex Virus Infection. *Front Microbiol* **8**, 2565 (2017). <https://doi.org:10.3389/fmicb.2017.02565>
- 102 Russell, T., Bleasdale, B., Hollinshead, M. & Elliott, G. Qualitative Differences in Capsidless L-Particles Released as a By-Product of Bovine Herpesvirus 1 and Herpes Simplex Virus 1 Infections. *J Virol* **92** (2018). <https://doi.org:10.1128/JVI.01259-18>
- 103 Tseng, C. C. & Li, C. S. Inactivation of viruses on surfaces by ultraviolet germicidal irradiation. *J Occup Environ Hyg* **4**, 400-405 (2007). <https://doi.org:10.1080/15459620701329012>
- 104 Rule Wigginton, K., Menin, L., Montoya, J. P. & Kohn, T. Oxidation of virus proteins during UV(254) and singlet oxygen mediated inactivation. *Environ Sci Technol* **44**, 5437-5443 (2010). <https://doi.org:10.1021/es100435a>
- 105 Kojima, M. *et al.* Irradiation by a Combination of Different Peak-Wavelength Ultraviolet-Light Emitting Diodes Enhances the Inactivation of Influenza A Viruses. *Microorganisms* **8** (2020). <https://doi.org:10.3390/microorganisms8071014>
- 106 Workman, A. & Jones, C. Productive infection and bICP0 early promoter activity of bovine herpesvirus 1 are stimulated by E2F1. *J Virol* **84**, 6308-6317 (2010). <https://doi.org:10.1128/JVI.00321-10>
- 107 Flores, E. F. & Donis, R. O. Isolation of a mutant MDBK cell line resistant to bovine viral diarrhea virus infection due to a block in viral entry. *Virology* **208**, 565-575 (1995). <https://doi.org:10.1006/viro.1995.1187>
- 108 Miller, C. G., Krummenacher, C., Eisenberg, R. J., Cohen, G. H. & Fraser, N. W. Development of a syngenic murine B16 cell line-derived melanoma susceptible to destruction by neuroattenuated HSV-1. *Mol Ther* **3**, 160-168 (2001). <https://doi.org:10.1006/mthe.2000.0240>
- 109 Keil, G. M., Hohle, C., Giesow, K. & Konig, P. Engineering glycoprotein B of bovine herpesvirus 1 to function as transporter for secreted proteins: a new protein expression approach. *J Virol* **79**, 791-799 (2005). <https://doi.org:10.1128/JVI.79.2.791-799.2005>
- 110 Plummer, G. & Lewis, B. Thermoinactivation of Herpes Simplex Virus and Cytomegalovirus. *J Bacteriol* **89**, 671-674 (1965). <https://doi.org:10.1128/jb.89.3.671-674.1965>
- 111 Hoffmann, G. *et al.* Monitoring the body temperature of cows and calves using video recordings from an infrared thermography camera. *Vet Res Commun* **37**, 91-99 (2013). <https://doi.org:10.1007/s11259-012-9549-3>
- 112 Dai, H. *et al.* Construction of BHV-1 UL41 Defective Virus Using the CRISPR/Cas9 System and Analysis of Viral Replication Properties. *Front Cell Infect Microbiol* **12**, 942987 (2022). <https://doi.org:10.3389/fcimb.2022.942987>

- 113 Gujar, S., Pol, J. G. & Kroemer, G. Heating it up: Oncolytic viruses make tumors 'hot' and suitable for checkpoint blockade immunotherapies. *Oncoimmunology* **7**, e1442169 (2018). <https://doi.org/10.1080/2162402X.2018.1442169>
- 114 Zhang, X. *et al.* Tumor Suppressor Gene XEDAR Promotes Differentiation and Suppresses Proliferation and Migration of Gastric Cancer Cells Through Upregulating the RELA/LXR $\alpha$  Axis and Deactivating the Wnt/ $\beta$ -Catenin Pathway. *Cell Transplantation* **30** (2021). <https://doi.org/10.1177/0963689721996346>
- 115 Tanikawa, C., Ri, C., Kumar, V., Nakamura, Y. & Matsuda, K. Crosstalk of EDA-A2/XEDAR in the p53 signaling pathway. *Mol Cancer Res* **8**, 855-863 (2010). <https://doi.org/10.1158/1541-7786.MCR-09-0484>
- 116 Fleith, R. C. *et al.* IFIT3 and IFIT2/3 promote IFIT1-mediated translation inhibition by enhancing binding to non-self RNA. *Nucleic Acids Res* **46**, 5269-5285 (2018). <https://doi.org/10.1093/nar/gky191>
- 117 Pidugu, V. K., Pidugu, H. B., Wu, M. M., Liu, C. J. & Lee, T. C. Emerging Functions of Human IFIT Proteins in Cancer. *Front Mol Biosci* **6**, 148 (2019). <https://doi.org/10.3389/fmolb.2019.00148>
- 118 Carlow DA, Teh SJ & HS, T. Specific antiviral activity demonstrated by TGTP, a member of a new family of interferon-induced GTPases. (1998). <https://doi.org/10.1006/biophys.1998.1615>
- 119 Cai, Y. *et al.* Interferon-Induced Transmembrane Protein 3 Shapes an Inflamed Tumor Microenvironment and Identifies Immuno-Hot Tumors. *Front Immunol* **12**, 704965 (2021). <https://doi.org/10.3389/fimmu.2021.704965>
- 120 Seillier, M., Peugeot, S., J. N. & Carrier, A. Antioxidant Role of p53 and of Its Target TP53INP1. *InTech* (2012). <https://doi.org/http://dx.doi.org/10.5772/50790>
- 121 Alibo, E. *et al.* P53 is a direct regulator of the immune co-stimulatory molecule CD80. (2021). <https://doi.org/10.1101/2021.05.24.445214>
- 122 Jang, J. S. *et al.* Rsad2 is necessary for mouse dendritic cell maturation via the IRF7-mediated signaling pathway. *Cell Death Dis* **9**, 823 (2018). <https://doi.org/10.1038/s41419-018-0889-y>
- 123 Lewis, M. W. *et al.* Enhancer RNA Transcription Is Essential for a Novel CSF1 Enhancer in Triple-Negative Breast Cancer. *Cancers (Basel)* **14** (2022). <https://doi.org/10.3390/cancers14071852>
- 124 Gordon, E. M., Ravicz, J. R., Liu, S., Chawla, S. P. & Hall, F. L. Cell cycle checkpoint control: The cyclin G1/Mdm2/p53 axis emerges as a strategic target for broad-spectrum cancer gene therapy - A review of molecular mechanisms for oncologists. *Mol Clin Oncol* **9**, 115-134 (2018). <https://doi.org/10.3892/mco.2018.1657>
- 125 Liu, M., Guo, S. & Stiles, J. K. The emerging role of CXCL10 in cancer (Review). *Oncol Lett* **2**, 583-589 (2011). <https://doi.org/10.3892/ol.2011.300>
- 126 Klepinin, A. *et al.* Adenylate Kinase and Metabolic Signaling in Cancer Cells. *Front Oncol* **10**, 660 (2020). <https://doi.org/10.3389/fonc.2020.00660>
- 127 Xu, H. *et al.* GBP3 promotes glioblastoma resistance to temozolomide by enhancing DNA damage repair. *Oncogene* **41**, 3876-3885 (2022). <https://doi.org/10.1038/s41388-022-02397-5>
- 128 Desai, S. D. ISG15: A double edged sword in cancer. *Oncoimmunology* **4**, e1052935 (2015). <https://doi.org/10.1080/2162402X.2015.1052935>



- 129 Tian, L. *et al.* IRGM1 enhances B16 melanoma cell metastasis through PI3K-Rac1 mediated epithelial mesenchymal transition. *Sci Rep* **5**, 12357 (2015).  
<https://doi.org:10.1038/srep12357>
- 130 King, K. Y. *et al.* Irgm1 protects hematopoietic stem cells by negative regulation of IFN signaling. *Blood* **118**, 1525-1533 (2011). <https://doi.org:10.1182/blood-2011-01-328682>
- 131 Lai, Y. Membrane transporters and the diseases corresponding to functional defects. (2013). <https://doi.org:https://doi.org/10.1533/9781908818287.1>
- 132 Saira, K., Zhou, Y. & Jones, C. The infected cell protein 0 encoded by bovine herpesvirus 1 (bICP0) induces degradation of interferon response factor 3 and, consequently, inhibits beta interferon promoter activity. *J Virol* **81**, 3077-3086 (2007).  
<https://doi.org:10.1128/JVI.02064-06>
- 133 Brownell, J. *et al.* Direct, interferon-independent activation of the CXCL10 promoter by NF-kappaB and interferon regulatory factor 3 during hepatitis C virus infection. *J Virol* **88**, 1582-1590 (2014). <https://doi.org:10.1128/JVI.02007-13>
- 134 Hanon, E. *et al.* Bovine herpesvirus 1-induced apoptotic cell death: role of glycoprotein D. *Virology* **257**, 191-197 (1999). <https://doi.org:10.1006/viro.1999.9620>
- 135 Gomez-Lopez, V. M. *et al.* Inactivation of Foodborne Viruses by UV Light: A Review. *Foods* **10** (2021). <https://doi.org:10.3390/foods10123141>
- 136 Alfson, K. J. *et al.* Particle-to-PFU ratio of Ebola virus influences disease course and survival in cynomolgus macaques. *J Virol* **89**, 6773-6781 (2015).  
<https://doi.org:10.1128/JVI.00649-15>
- 137 McCormick, W. & Mermel, L. A. The basic reproductive number and particle-to-plaque ratio: comparison of these two parameters of viral infectivity. *Virol J* **18**, 92 (2021).  
<https://doi.org:10.1186/s12985-021-01566-4>
- 138 Sayedahmed EE & SK., M. A potential approach for assessing the quality of human and nonhuman adenoviral vector preparations. (2020). [https://doi.org:84\(4\):314-318](https://doi.org:84(4):314-318)
- 139 Ma, Y., Zhang, Y. & Zhu, L. Role of neutrophils in acute viral infection. *Immunity, Inflammation and Disease* **9**, 1186-1196 (2021). <https://doi.org:10.1002/iid3.500>
- 140 Jenne, C. N. *et al.* Neutrophils recruited to sites of infection protect from virus challenge by releasing neutrophil extracellular traps. *Cell Host Microbe* **13**, 169-180 (2013).  
<https://doi.org:10.1016/j.chom.2013.01.005>
- 141 Song, B., Shiromoto, Y., Minakuchi, M. & Nishikura, K. The role of RNA editing enzyme ADAR1 in human disease. *Wiley Interdiscip Rev RNA* **13**, e1665 (2022).  
<https://doi.org:10.1002/wrna.1665>
- 142 Lamers, M. M., van den Hoogen, B. G. & Haagmans, B. L. ADAR1: "Editor-in-Chief" of Cytoplasmic Innate Immunity. *Front Immunol* **10**, 1763 (2019).  
<https://doi.org:10.3389/fimmu.2019.01763>
- 143 Hartner, J. C. *et al.* Liver disintegration in the mouse embryo caused by deficiency in the RNA-editing enzyme ADAR1. *J Biol Chem* **279**, 4894-4902 (2004).  
<https://doi.org:10.1074/jbc.M311347200>
- 144 Hartner, J. C., Walkley, C. R., Lu, J. & Orkin, S. H. ADAR1 is essential for the maintenance of hematopoiesis and suppression of interferon signaling. *Nat Immunol* **10**, 109-115 (2009). <https://doi.org:10.1038/ni.1680>
- 145 Kanno, S. *et al.* Susceptibility to cytosine arabinoside (Ara-C)-induced cytotoxicity in human leukemia cell lines. *Toxicol Lett* **152**, 149-158 (2004).  
<https://doi.org:10.1016/j.toxlet.2004.04.014>

- 146 Bleasdale, B. Novel Envelopment Dynamics in BHV-1 Assembly. (2015).  
[https://doi.org:https://doi.org/10.25560/49227](https://doi.org/10.25560/49227)
- 147 Prasanna, T. & Faruqi, A. *Cytarabine*. (2022).